NASA Contractor Report 195054

ICASE Report No. 95-15

ICASE

A REVIEW OF REYNOLDS STRESS MODELS FOR TURBULENT SHEAR FLOWS

Charles G. Speziale

Contract No. NAS1-19480
March 1995

Institute for Computer Applications in Science and Engineering
NASA Langley Research Center
Hampton, VA 23681-0001

Operated by Universities Space Research Association

A REVIEW OF REYNOLDS STRESS MODELS FOR TURBULENT SHEAR FLOWS

*Charles G. Speziale**

Aerospace & Mechanical Engineering Department
Boston University
Boston, Massachusetts 02215

Abstract

A detailed review of recent developments in Reynolds stress modeling for incompressible turbulent shear flows is provided. The mathematical foundations of both two-equation models and full second-order closures are explored in depth. It is shown how these models can be systematically derived for two-dimensional mean turbulent flows that are close to equilibrium. A variety of examples are provided to demonstrate how well properly calibrated versions of these models perform for such flows. However, substantial problems remain for the description of more complex turbulent flows where there are large departures from equilibrium. Recent efforts to extend Reynolds stress models to non-equilibrium turbulent flows are discussed briefly along with the major modeling issues relevant to practical Naval Hydrodynamics applications.

*Research was supported by the National Aeronautics and Space Administration under NASA Contract No. NAS1-19480 while the author was in residence at the Institute for Computer Applications in Science and Engineering (ICASE), NASA Langley Research Center, Hampton, VA 23681-0001. Funding was also provided by the Office of Naval Research under Grant N00014-94-1-0088 (ARI on Nonequilibrium Turbulence, Dr. L. P. Purtell, Program Officer).

1. Introduction

Turbulent shear flows are of central importance for a variety of Naval Hydrodynamics applications ranging from flow around submerged bodies to free surface flows. Most of these turbulent flows are at extremely high Reynolds numbers – and in complex geometrical flow configurations – where the application of direct or large-eddy simulations are all but impossible for the foreseeable future. Reynolds stress models are likely to remain the only technologically feasible approach for the solution of these problems for the next few decades to come, if not beyond (see Speziale [1]).

It is widely believed that Reynolds stress models are completely ad hoc, having no formal connection with solutions of the full Navier-Stokes equations for turbulent flows. While this belief is largely warranted for the older eddy viscosity models of turbulence, it constitutes a far too pessimistic assessment of the current generation of Reynolds stress closures. It will be shown how second-order closure models and two equation models with an anisotropic eddy viscosity can be systematically derived from the Navier-Stokes equations when one overriding assumption is made: the turbulence is locally homogeneous and in equilibrium. Moderate departures from equilibrium – where there are weak inhomogeneous effects – can then be accounted for in a relatively straightforward fashion.

A brief review of zero and one equation models based on the Boussinesq eddy viscosity hypothesis will first be given in order to provide a perspective on the earlier approaches to Reynolds stress modeling. However, it will then be argued that since turbulent flows contain length and time scales which can change dramatically from one flow configuration to the next, two-equation models constitute the minimum level of closure that is physically acceptable. Typically, modeled transport equations are solved for the turbulent kinetic energy and dissipation rate from which the turbulent length and time scales are built up; this obviates the need to specify these scales in an ad hoc fashion for different flows. While two-equation models represent the minimum acceptable level of closure, second-order closure models constitute the highest level of closure that is currently feasible from a practical computational standpoint. It will be shown how the former models follow from the latter in the equilibrium limit of homogeneous turbulence (see Speziale, Sarkar and Gatski [2] and Gatski and Speziale [3]). However, it will be demonstrated that the two-equation models which are formally consistent with second-order closures have an *anisotropic eddy viscosity with strain-dependent coefficients* – features that the most commonly used models do not possess.

For turbulent flows that are only weakly inhomogeneous, full Reynolds stress closures can then be constructed by the addition of turbulent diffusion terms that are formally derived via a gradient transport hypothesis. Properly calibrated versions of these models are found to

yield a surprisingly good description of a wide range of two-dimensional mean turbulent flows that are near equilibrium. In particular, plane turbulent shear flows are accurately described with the stabilizing or destabilizing effect of a system rotation predicted in a manner that is quantitatively consistent with hydrodynamic stability theory. However, existing second-order closures are not currently capable of properly describing turbulent flows that are far from equilibrium and have major problems with wall-bounded turbulent flows. In regard to the latter point, it will be argued that we do not currently know how to properly integrate second-order closure models to a solid boundary with the no-slip condition applied. A variety of ad hoc wall damping functions are currently used that depend on the unit normal to (and/or the distance from) the wall – a feature that makes it virtually impossible to reliably apply these models in complex geometries. Consequently, in many applications of second-order closures to wall-bounded turbulence, the integration is carried out by matching to law of the wall boundary conditions, which do not formally apply to complex turbulent flows. The really disturbing feature here is that many of the commonly used second-order closures are not even capable of reproducing law of the wall results for an equilibrium turbulent boundary layer unless an ad hoc wall reflection term is added. This term typically depends inversely on the distance from the wall, further compromising the ability to apply these models in complex geometries. Entirely new approaches to the modeling of complex non-equilibrium and wall-bounded turbulent flows will be discussed briefly.

A variety of illustrative examples involving turbulent shear flows will be provided in order to amplify the central points discussed in this paper. In addition, a special effort will be made to address the crucial issues in turbulence modeling that are relevant to practical Naval Hydrodynamics applications.

2. Basic Equations of Turbulence

We will consider the incompressible turbulent flow of a viscous fluid under isothermal conditions. The velocity field v_i and kinematic pressure P are solutions of the Navier-Stokes and continuity equations given by

$$\frac{\partial v_i}{\partial t} + v_j \frac{\partial v_i}{\partial x_j} = -\frac{\partial P}{\partial x_i} + \nu \nabla^2 v_i \tag{1}$$

$$\frac{\partial v_i}{\partial x_i} = 0 \tag{2}$$

where ν is the kinematic viscosity and the Einstein summation convention applies to repeated indices. As in all traditional studies of turbulence modeling, the velocity and kinematic pressure are decomposed into mean and fluctuating parts as follows:

$$v_i = \overline{v}_i + u_i, \quad P = \overline{P} + p \tag{3}$$

where an overbar represents a Reynolds average. This Reynolds average can take a variety of forms for any flow variable ϕ:

Homogeneous Turbulence

$$\overline{\phi} = \lim_{V\to\infty} \frac{1}{V}\int_V \phi(\mathbf{x},t)d^3x \tag{4}$$

$$\overline{\phi} = \overline{\phi}(t) \quad \text{(Spatial Average)}$$

Statistically Steady Turbulence

$$\overline{\phi} = \lim_{T\to\infty} \frac{1}{T}\int_0^T \phi(\mathbf{x},t)dt \tag{5}$$

$$\overline{\phi} = \overline{\phi}(\mathbf{x}) \quad \text{(Time Average)}$$

General Turbulence

$$\overline{\phi} = \lim_{N\to\infty} \frac{1}{N}\sum_{\alpha=1}^{N} \phi^{(\alpha)}(\mathbf{x},t) \tag{6}$$

$$\overline{\phi} = \overline{\phi}(\mathbf{x},t) \quad \text{(Ensemble Average)}.$$

In (6), α represents a given realization of the turbulence.

The *Ergodic Hypothesis* is assumed to apply. In a homogeneous turbulence,

$$\overline{\phi}_{\text{ensemble}} = \overline{\phi}_{\text{spatial}} \tag{7}$$

whereas in a statistically steady turbulence,

$$\overline{\phi}_{\text{ensemble}} = \overline{\phi}_{\text{time}}. \tag{8}$$

For general turbulent flows that are neither statistically steady nor homogeneous, ensemble averages should be used (cf. Hinze [4] for a detailed discussion of these issues).

The Reynolds-averaged Navier-Stokes and continuity equations take the form (cf. Hinze [4])

$$\frac{\partial \overline{v}_i}{\partial t} + \overline{v}_j\frac{\partial \overline{v}_i}{\partial x_j} = -\frac{\partial \overline{P}}{\partial x_i} + \nu\nabla^2\overline{v}_i - \frac{\partial \tau_{ij}}{\partial x_j} \tag{9}$$

$$\frac{\partial \overline{v}_i}{\partial x_i} = 0 \tag{10}$$

where

$$\tau_{ij} \equiv \overline{u_i u_j} \tag{11}$$

is the Reynolds stress tensor.

The Reynolds-averaged Navier-Stokes equation is not closed until a model is provided that ties the Reynolds stress tensor τ_{ij} to the global history of the mean velocity $\overline{v}_i$ in a physically consistent fashion. In mathematical terms, τ_{ij} is a functional of the global history of the mean velocity field, i.e.,

$$\tau_{ij}(\mathbf{x},t) = \mathcal{F}_{ij}[\overline{\mathbf{v}}(\mathbf{x}',t');\mathbf{x},t] \quad \mathbf{x}'\epsilon\mathcal{V},\ t'\epsilon(-\infty,t) \tag{12}$$

where $\mathcal{F}_{ij}[\ \cdot\ ]$ denotes a functional over space and time, and $\mathcal{V}$ represents the fluid volume. In (12), it is understood that there is an implicit dependence on the initial and boundary conditions for u_i and, hence, on those for the entire hierarchy of moments constructed from the fluctuating velocity. For the construction of Reynolds stress closures, it is typically assumed that the initial and boundary conditions for any turbulence correlations beyond the Reynolds stress tensor and dissipation rate merely serve to set the level of the length and time scales (see Lumley [5] and Speziale [1]).

3. Zero and One Equation Models

The Reynolds stress tensor can be decomposed into isotropic and deviatoric parts as follows:

$$\tau_{ij} = \frac{2}{3}K\delta_{ij} + {}_D\tau_{ij} \tag{13}$$

where the deviatoric part ${}_D\tau_{ij}$ is a symmetric and traceless tensor. Virtually all of the commonly used Reynolds stress models in this class are based on the Boussinesq hypothesis where it is assumed that

$${}_D\tau_{ij} = -\nu_T\left(\frac{\partial\overline{v}_i}{\partial x_j} + \frac{\partial\overline{v}_j}{\partial x_i}\right) \tag{14}$$

given that ν_T is the eddy viscosity. For most incompressible turbulent flows, the isotropic part of the Reynolds stress tensor $\left(\frac{2}{3}K\right)$ is not needed for the determination of the mean velocity field since it can simply be absorbed into the mean pressure $\overline{P}$ in (9).

The eddy viscosity can be written as

$$\nu_T = \frac{\ell_0^2}{t_0} \tag{15}$$

where ℓ_0 is the turbulent length scale and t_0 is the turbulent time scale – quantities that can vary dramatically with space and time for a given turbulent flow. In *zero equation models*, both ℓ_0 and t_0 are specified algebraically by empirical means. The first successful zero equation model based on the Boussinesq eddy viscosity hypothesis was Prandtl's mixing length theory (see Prandtl [6]). In Prandtl's mixing length theory,

$$\nu_T = \ell_0^2\left|\frac{d\overline{u}}{dy}\right| \tag{16}$$

where $\ell_0 = \kappa y$ is the mixing length, κ is the von Kármán constant, and y is the normal distance from a solid boundary. This representation is only formally valid for thin turbulent shear flows – near a wall – where the mean velocity is of the simple unidirectional form $\overline{\mathbf{v}} = \overline{u}(y)\mathbf{i}$.

Several decades later, this simple mixing length model was generalized to multi-dimensional turbulent flows. Three alternative tensorially invariant forms have been proposed:

Smagorinsky [7] Model

$$\nu_T = \ell_0^2 (2\overline{S}_{ij}\overline{S}_{ij})^{1/2} \tag{17}$$

Cebeci-Smith [8] Model

$$\nu_T = \ell_0^2 \left(\frac{\partial \overline{v}_i}{\partial x_j} \frac{\partial \overline{v}_i}{\partial x_j} \right)^{1/2} \tag{18}$$

Baldwin-Lomax [9] Model

$$\nu_T = \ell_0^2 (\overline{\omega}_i \overline{\omega}_i)^{1/2} \tag{19}$$

where $\overline{S}_{ij} = \frac{1}{2}(\partial \overline{v}_i/\partial x_j + \partial \overline{v}_j/\partial x_i)$ is the mean rate of strain tensor and $\overline{\boldsymbol{\omega}} = \nabla \times \overline{\mathbf{v}}$ is the mean vorticity vector. The former model has been primarily used as a subgrid scale model for large-eddy simulations whereas the latter two models have been used for Reynolds-averaged Navier-Stokes computations in aerodynamics. Each of these models reduces to the simple mixing length formula (16) in the thin shear flow limit. However, they suffer from the same deficiency as the original mixing length model in their need for an ad hoc specification of the turbulent length scale ℓ_0 – a task that is all but impossible to do reliably in complex turbulent flows.

Beyond the length scale specification problem with zero equation models, there is another criticism that can be raised: it is not physically consistent to build up the turbulent velocity scale from the mean velocity gradients as done in (17) - (19). The proper measure of the turbulent velocity scale is the intensity of the turbulent fluctuations (i.e., we should take $v_0 = K^{1/2}$ where $v_0 \equiv \ell_0/t_0$). Hence, a more physically consistent representation for the eddy viscosity is given by

$$\nu_T = K^{1/2}\ell_0. \tag{20}$$

Prandtl [10] – who expanded on many of the earlier ideas of Kolmogorov [11] – developed a one-equation model based on (20) wherein a modeled transport equation for the turbulent kinetic energy was solved. Subsequent to this early work, a variety of researchers have proposed one-equation models along these lines for near-wall turbulent flows (cf. Norris and Reynolds [12] and Rodi, Mansour and Michelassi [13]).

One-equation models based on the solution of a modeled transport equation for the turbulent kinetic energy still suffer from one of the major deficiencies of mixing length models: they require the ad hoc specification of the turbulent length scale which is virtually impossible to do reliably in complex three-dimensional turbulent flows. Recently, one-equation models have been proposed based on the solution of a modeled transport equation for the eddy viscosity ν_T (see Baldwin and Barth [14] and Spalart and Allmaras [15]). These models do alleviate the problem of having to specify the turbulent length scale in the definition of the eddy viscosity (20). Nonetheless, an ad hoc specification of length scale must be made in the destruction term within the modeled transport equation for ν_T which depends empirically on the distance from the wall.

This leads us to one of the central points of this paper: the turbulent length and time scales (ℓ_0, t_0) are *not* universal; they depend strongly on the flow configuration under consideration. Consequently, *two-equation models* – wherein transport equations are solved for two independent quantities that are directly related to the turbulent length and time scales – represent the *minimum acceptable level of closure.* In the most common approach, the turbulent length and time scales are built up from the turbulent kinetic energy K and dissipation rate ε (i.e., $\ell_0 \propto K^{3/2}/\varepsilon$, $t_0 \propto K/\varepsilon$) with modeled transport equations solved for K and ε. These two-equation models should be formulated with a properly invariant *anisotropic eddy viscosity* that is nonlinear in the mean velocity gradients. The standard Boussinesq eddy viscosity hypothesis makes it impossible to properly describe turbulent flows with: (a) body force effects arising from a system rotation or from streamline curvature, and (b) flow structures generated by normal Reynolds stress anisotropies (e.g., secondary flows in non-circular ducts).

At this point, it would be useful to comment on the most sophisticated level of Reynolds stress closure that is now practical. Limitations in computer capacity, and issues of numerical stiffness, appear to make *second-order closure models* – wherein modeled transport equations are solved for the individual components of the Reynolds stress tensor along with a scale equation – *the highest level of closure* that is currently feasible for practical computations.

4. Turbulent Transport Equations

The transport equation for the fluctuating velocity u_i, which is obtained by subtracting (9) from (1), takes the form

$$\begin{aligned} \frac{\partial u_i}{\partial t} + \overline{v}_j \frac{\partial u_i}{\partial x_j} \;=\; & -u_j \frac{\partial u_i}{\partial x_j} - u_j \frac{\partial \overline{v}_i}{\partial x_j} - \frac{\partial p}{\partial x_i} \\ & + \nu \nabla^2 u_i + \frac{\partial \tau_{ij}}{\partial x_j}. \end{aligned} \tag{21}$$

This equation can be written in operator form as

$$\mathcal{N}u_i = 0. \tag{22}$$

The Reynolds stress transport equation is obtained by constructing the second moment

$$\overline{u_i \mathcal{N} u_j + u_j \mathcal{N} u_i} = 0. \tag{23}$$

Its full form is given by (cf. Hinze [4])

$$\begin{aligned} \frac{\partial \tau_{ij}}{\partial t} + \overline{v}_k \frac{\partial \tau_{ij}}{\partial x_k} = & -\tau_{ik}\frac{\partial \overline{v}_j}{\partial x_k} - \tau_{jk}\frac{\partial \overline{v}_i}{\partial x_k} + \Phi_{ij} \\ & -\varepsilon_{ij} - \frac{\partial C_{ijk}}{\partial x_k} + \nu \nabla^2 \tau_{ij}. \end{aligned} \tag{24}$$

In (24),

$$\Phi_{ij} \equiv \overline{p\left(\frac{\partial u_i}{\partial x_j} + \frac{\partial u_j}{\partial x_i}\right)} \tag{25}$$

$$\varepsilon_{ij} \equiv 2\nu \overline{\frac{\partial u_i}{\partial x_k}\frac{\partial u_j}{\partial x_k}} \tag{26}$$

$$C_{ijk} \equiv \overline{u_i u_j u_k} + \overline{p u_i}\delta_{jk} + \overline{p u_j}\delta_{ik} \tag{27}$$

are, respectively, the pressure-strain correlation, the dissipation rate tensor and the turbulent diffusion correlation.

The transport equation for the turbulent kinetic energy $K \equiv \frac{1}{2}\tau_{ii}$ is obtained by contracting (24):

$$\frac{\partial K}{\partial t} + \overline{v}_j \frac{\partial K}{\partial x_j} = \mathcal{P} - \varepsilon - \frac{\partial}{\partial x_j}\left(\frac{1}{2}\overline{u_i u_i u_j} + \overline{p u_j}\right) + \nu \nabla^2 K \tag{28}$$

where

$$\mathcal{P} \equiv -\tau_{ij}\frac{\partial \overline{v}_i}{\partial x_j} \tag{29}$$

$$\varepsilon \equiv \nu \overline{\frac{\partial u_i}{\partial x_j}\frac{\partial u_i}{\partial x_j}} \tag{30}$$

are, respectively, the turbulence production and the turbulent dissipation rate. By constructing the moment

$$2\nu \overline{\frac{\partial u_i}{\partial x_j}\frac{\partial}{\partial x_j}(\mathcal{N}u_i)} = 0, \tag{31}$$

a transport equation for the turbulent dissipation rate ε can be obtained. This equation takes the form [1]

$$\frac{\partial \varepsilon}{\partial t} + \overline{v}_i \frac{\partial \varepsilon}{\partial x_i} = \mathcal{P}_\varepsilon - \Phi_\varepsilon + \mathcal{D}_\varepsilon + \nu \nabla^2 \varepsilon \tag{32}$$

where

$$\mathcal{P}_\varepsilon = -2\nu\overline{\frac{\partial u_k}{\partial x_i}\frac{\partial u_k}{\partial x_j}\frac{\partial \overline{v}_i}{\partial x_j}} - 2\nu\overline{\frac{\partial u_i}{\partial x_k}\frac{\partial u_j}{\partial x_k}\frac{\partial \overline{v}_i}{\partial x_j}} \tag{33}$$

$$-2\nu\overline{\frac{\partial u_k}{\partial x_i}\frac{\partial u_k}{\partial x_j}\frac{\partial u_i}{\partial x_j}} - 2\nu\overline{u_k\frac{\partial u_i}{\partial x_j}}\frac{\partial^2 \overline{v}_i}{\partial x_j \partial x_k}$$

$$\Phi_\varepsilon = 2\nu^2\overline{\frac{\partial^2 u_i}{\partial x_j \partial x_k}\frac{\partial^2 u_i}{\partial x_j \partial x_k}} \tag{34}$$

$$\mathcal{D}_\varepsilon = -2\nu\frac{\partial}{\partial x_j}\left(\overline{\frac{\partial p}{\partial x_i}\frac{\partial u_j}{\partial x_i}}\right) - \nu\frac{\partial}{\partial x_j}\left(\overline{u_j\frac{\partial u_i}{\partial x_k}\frac{\partial u_i}{\partial x_k}}\right) \tag{35}$$

are, respectively, the production, destruction and turbulent diffusion of dissipation.

Both two-equation models and second-order closure models are obtained by modeling the Reynolds stress transport equation (24) and the dissipation rate transport equation (32). *Second-order closures* are obtained by modeling the *full* Reynolds stress transport equation. *Two-equation models* are formally obtained by assuming that the turbulence is locally homogeneous and in equilibrium; the Reynolds stress anisotropies are then derived algebraically from (24) and a modeled version of (28) for the turbulent kinetic energy is solved.

5. Two-Equation Models

It will now be shown how two-equation models can be systematically derived from the Reynolds stress transport equation. As alluded to earlier, two-equation models – with an algebraic representation for the Reynolds stresses – are obtained by assuming that the turbulence is locally homogeneous and in equilibrium. Hence, we start with the Reynolds stress transport equation for homogeneous turbulence given by:

$$\dot{\tau}_{ij} = -\tau_{ik}\frac{\partial \overline{v}_j}{\partial x_k} - \tau_{jk}\frac{\partial \overline{v}_i}{\partial x_k} + \Phi_{ij} - \varepsilon_{ij}. \tag{36}$$

Since, the fluctuating pressure p is a solution of the Poisson equation

$$\nabla^2 p = -\frac{\partial u_i}{\partial x_j}\frac{\partial u_j}{\partial x_i} - 2\frac{\partial \overline{v}_i}{\partial x_j}\frac{\partial u_j}{\partial x_i} \tag{37}$$

it follows that the pressure-strain correlation can be written in the form

$$\Phi_{ij} = A_{ij} + M_{ijkl}\frac{\partial \overline{v}_k}{\partial x_l} \tag{38}$$

In (38),

$$A_{ij} = \frac{1}{4\pi}\overline{\int_{-\infty}^{\infty}\int\int\int \frac{1}{|\mathbf{x}-\mathbf{x}^*|}\frac{\partial u_k^*}{\partial x_l^*}\frac{\partial u_l^*}{\partial x_k^*}\left(\frac{\partial u_i}{\partial x_j} + \frac{\partial u_j}{\partial x_i}\right) d^3x^*} \tag{39}$$

$$M_{ijkl} = \frac{1}{2\pi} \overline{\int\int\int_{-\infty}^{\infty} \frac{1}{|\mathbf{x}-\mathbf{x}^*|} \frac{\partial u_l^*}{\partial x_k^*} \left(\frac{\partial u_i}{\partial x_j} + \frac{\partial u_j}{\partial x_i} \right) d^3x^*} \tag{40}$$

are, respectively, the slow and rapid terms which are obtained by implementing the Green's function solution of (37) for an infinite flow domain.

In the developments to follow, extensive use will be made of the Reynolds stress and dissipation rate anisotropy tensors defined as

$$b_{ij} = \frac{\tau_{ij} - \frac{2}{3}K\delta_{ij}}{2K} \tag{41}$$

$$d_{ij} = \frac{\varepsilon_{ij} - \frac{2}{3}\varepsilon\delta_{ij}}{2\varepsilon} \tag{42}$$

respectively (see Lumley [16] and Reynolds [17]). Furthermore, use will be made of the transport equation for the turbulent kinetic energy which is exact for homogeneous turbulence:

$$\dot{K} = P - \varepsilon \tag{43}$$

Eq. (43) is obtained by contracting (36). The direct substitution of (38) - (42) into (36) yields the Reynolds stress transport equation

$$\begin{aligned} \dot{b}_{ij} = &-\frac{2}{3}\overline{S}_{ij} - \left(b_{ik}\frac{\partial \overline{v}_j}{\partial x_k} + b_{jk}\frac{\partial \overline{v}_i}{\partial x_k} - \frac{2}{3}b_{kl}\frac{\partial \overline{v}_k}{\partial x_l}\delta_{ij} \right) \\ &+\frac{1}{2K}\left(\varepsilon\mathcal{A}_{ij} + K\mathcal{M}_{ijkl}\frac{\partial \overline{v}_k}{\partial x_l} \right) - \frac{\varepsilon}{K}d_{ij} \end{aligned} \tag{44}$$

given in terms of the anisotropy tensors alone. In (44), $\mathcal{A}_{ij} \equiv A_{ij}/\varepsilon$ and $\mathcal{M}_{ijkl} \equiv M_{ijkl}/K$ are the dimensionless slow and rapid pressure-strain terms.

The fundamental assumptions underlying two-equation models are that the turbulence is *locally* homogeneous and an equilibrium state is reached where

$$b_{ij}, d_{ij}, \mathcal{A}_{ij}, \mathcal{M}_{ijkl}, \frac{K}{\varepsilon}$$

attain constant values that are largely independent of the initial conditions. In general, A_{ij} and M_{ijkl} are functionals, in wavevector space $\mathbf{k}$, of the energy spectrum tensor $E_{ij}(\mathbf{k},t)$ where

$$\tau_{ij} = \int\int\int_{-\infty}^{\infty} E_{ij}(\mathbf{k},t)d^3k \tag{45}$$

(cf. Reynolds [17]). This has prompted turbulence modelers to construct one-point models for $\mathcal{A}_{ij}$ and $\mathcal{M}_{ijkl}$ of the form (Lumley [16])

$$\mathcal{A}_{ij} = \mathcal{A}_{ij}(\mathbf{b}), \quad \mathcal{M}_{ijkl} = \mathcal{M}_{ijkl}(\mathbf{b}). \tag{46}$$

It should be said at the outset that models of the form (46) cannot be expected to apply to general homogeneous turbulent flows since nonlocal effects in wavevector space are neglected; it is well known that M_{ijkl} is of the form (cf. Reynolds [17])

$$M_{ijkl} \sim \int_{-\infty}^{\infty}\int\int \frac{k_i k_j}{k^2} E_{kl}(\mathbf{k},t) d^3k. \tag{47}$$

However, for homogeneous turbulent flows that are in equilibrium, there is evidence to suggest that $\mathcal{A}_{ij}, \mathcal{M}_{ijkl}$ and b_{ij} achieve constant values that are independent of the initial conditions as alluded to earlier (homogeneous shear flow represents a prime example; see Tavoularis and Corrsin [18]). Any constant tensor can be written as a finite expansion in three linearly independent vectors that are also constant. Since b_{ij} is a symmetric tensor, its eigenvectors are linearly independent; hence, (46) is expected to be formally valid for a homogeneous turbulence that achieves this type of structural equilibrium.

Speziale, Sarkar and Gatski [2] showed that for *two-dimensional* mean turbulent flows that are homogeneous and in equilibrium, the pressure-strain correlation reduces to the simple general form:

$$\begin{aligned}
\Phi_{ij} &= \varepsilon \mathcal{A}_{ij}(\mathbf{b}) + K\mathcal{M}_{ijkl}(\mathbf{b})\frac{\partial \overline{v}_k}{\partial x_l} \\
&= -C_1 \varepsilon b_{ij} + C_1^* \varepsilon \left(b_{ik}b_{kj} - \frac{1}{3} b_{mn}b_{mn}\delta_{ij} \right) \\
&\quad + C_2 K \overline{S}_{ij} + C_3 K \left(b_{ik}\overline{S}_{jk} + b_{jk}\overline{S}_{ik} \right. \\
&\quad \left. - \frac{2}{3} b_{kl}\overline{S}_{kl}\delta_{ij} \right) + C_4 K (b_{ik}\overline{\omega}_{jk} + b_{jk}\overline{\omega}_{ik})
\end{aligned} \tag{48}$$

where

$$\overline{S}_{ij} = \frac{1}{2}\left(\frac{\partial \overline{v}_i}{\partial x_j} + \frac{\partial \overline{v}_j}{\partial x_i} \right) \tag{49}$$

$$\overline{\omega}_{ij} = \frac{1}{2}\left(\frac{\partial \overline{v}_i}{\partial x_j} - \frac{\partial \overline{v}_j}{\partial x_i} \right) \tag{50}$$

are, respectively, the mean rate of strain tensor and the mean vorticity tensor. In (48), $C_1 - C_4$ are constants that are not necessarily universal; in principal, their specific numerical values can vary from one flow to the next. However, it is encouraging to note that, consistent with its definition (47), the basis expansion (48) has a rapid part that is linear in τ_{ij} and, hence, linear in the energy spectrum tensor. It is only in the limit of two-dimensional mean turbulent flows that the general basis expansion for $(46)_2$ satisfies this linear consistency condition – a result of the fact that II, III and b_{33} achieve universal equilibrium

values in the two-dimensional limit (Speziale, Sarkar and Gatski [2]). For uniformly strained turbulent flows near equilibrium, there is substantial evidence from physical and numerical experiments to suggest that the quadratic return term in (48) (with coefficient C_1^*) can be neglected without introducing an appreciable error. Then, the representation (48) becomes completely *linear* in the Reynolds stress tensor. This allows for the superposition of solutions and maintains consistency with the linearity of the rapid pressure-strain correlation in the energy spectrum tensor – a property that follows from its definition as stated above. In the opinion of the author, this constitutes the primary reason for the relative success that (46) has had in the description of two-dimensional mean turbulent flows that are near equilibrium. The applicability of (46) to non-equilibrium turbulent flows or to three-dimensional mean turbulent flows is highly debatable. In regard to the latter case, the general basis representation for $(46)_2$ is highly nonlinear in b_{ij} (see Lumley [16], Reynolds [17] and Speziale [1]) – and, therefore, nonlinear in the energy spectrum tensor – in violation of (47).

If we neglect the anisotropy of dissipation, then in the equilibrium limit where $\dot{b}_{ij} = 0$, Eq. (44) reduces to the following linear system of algebraic equations (see Gatski and Speziale [3]):

$$\begin{aligned} b_{ij}^* \;=\; & -\overline{S}_{ij}^* - b_{ik}^*\overline{S}_{jk}^* - b_{jk}^*\overline{S}_{ik}^* + \frac{2}{3}b_{kl}^*\overline{S}_{kl}^*\delta_{ij} \\ & + b_{ik}^*\overline{W}_{kj}^* + b_{jk}^*\overline{W}_{ki}^* \end{aligned} \tag{51}$$

where

$$\overline{S}_{ij}^* = \frac{1}{2}g\frac{K}{\varepsilon}(2 - C_3)\overline{S}_{ij} \tag{52}$$

$$\overline{W}_{ij}^* = \frac{1}{2}g\frac{K}{\varepsilon}(2 - C_4)\overline{\omega}_{ij} \tag{53}$$

$$b_{ij}^* = \left(\frac{C_3 - 2}{C_2 - \frac{4}{3}}\right) b_{ij} \tag{54}$$

$$g = \left(\frac{C_1}{2} + \frac{\mathcal{P}}{\varepsilon} - 1\right)^{-1}. \tag{55}$$

For turbulent flows in non-inertial frames of reference, Coriolis terms must be added to the right-hand-side of (44) along with a non-inertial correction to the pressure-strain correlation model (48). As shown by Gatski and Speziale [3], these terms can be accounted for *exactly* by simply replacing (53) with the extended expression

$$\overline{W}_{ij}^* = \frac{1}{2}g\frac{K}{\varepsilon}(2 - C_4)\left[\overline{\omega}_{ij} + \left(\frac{C_4 - 4}{C_4 - 2}\right) e_{mji}\Omega_m\right] \tag{56}$$

where e_{mji} is the permutation tensor and Ω_m is the angular velocity of the reference frame (in an inertial frame of reference, where $\Omega_m = 0$, the expression (56) reduces to (53)).

Equation (51) constitutes a set of linear algebraic equations for the determination of b_{ij}^* in terms of $\overline{S}_{ij}^*$ and $\overline{W}_{ij}^*$; the solution to (51) is of the general mathematical form

$$\mathbf{b}^* = \mathbf{f}(\overline{\mathbf{S}}^*, \overline{\mathbf{W}}^*). \tag{57}$$

As first suggested by Pope [19], the general solution to the implicit algebraic stress equation (51) is of the form:

$$\mathbf{b}^* = \sum_{\lambda=1}^{10} G^{(\lambda)} \mathbf{T}^{(\lambda)} \tag{58}$$

where

$$\begin{aligned}
&\mathbf{T}^{(1)} = \overline{\mathbf{S}}^*, && \mathbf{T}^{(6)} = \overline{\mathbf{W}}^{*2}\overline{\mathbf{S}}^* + \overline{\mathbf{S}}^*\overline{\mathbf{W}}^{*2} - \tfrac{2}{3}\{\overline{\mathbf{S}}^*\overline{\mathbf{W}}^{*2}\}\mathbf{I} \\
&\mathbf{T}^{(2)} = \overline{\mathbf{S}}^*\overline{\mathbf{W}}^* - \overline{\mathbf{W}}^*\overline{\mathbf{S}}^*, && \mathbf{T}^{(7)} = \overline{\mathbf{W}}^*\overline{\mathbf{S}}^*\overline{\mathbf{W}}^{*2} - \overline{\mathbf{W}}^{*2}\overline{\mathbf{S}}^*\overline{\mathbf{W}}^* \\
&\mathbf{T}^{(3)} = \overline{\mathbf{S}}^{*2} - \tfrac{1}{3}\{\overline{\mathbf{S}}^{*2}\}\mathbf{I}, && \mathbf{T}^{(8)} = \overline{\mathbf{S}}^*\overline{\mathbf{W}}^*\overline{\mathbf{S}}^{*2} - \overline{\mathbf{S}}^{*2}\overline{\mathbf{W}}^*\overline{\mathbf{S}}^* \\
&\mathbf{T}^{(4)} = \overline{\mathbf{W}}^{*2} - \tfrac{1}{3}\{\overline{\mathbf{W}}^{*2}\}\mathbf{I}, && \mathbf{T}^{(9)} = \overline{\mathbf{W}}^{*2}\overline{\mathbf{S}}^{*2} + \overline{\mathbf{S}}^{*2}\overline{\mathbf{W}}^{*2} - \tfrac{2}{3}\{\overline{\mathbf{S}}^{*2}\overline{\mathbf{W}}^{*2}\}\mathbf{I} \\
&\mathbf{T}^{(5)} = \overline{\mathbf{W}}^*\overline{\mathbf{S}}^{*2} - \overline{\mathbf{S}}^{*2}\overline{\mathbf{W}}^*, && \mathbf{T}^{(10)} = \overline{\mathbf{W}}^*\overline{\mathbf{S}}^{*2}\overline{\mathbf{W}}^{*2} - \overline{\mathbf{W}}^{*2}\overline{\mathbf{S}}^{*2}\overline{\mathbf{W}}^*
\end{aligned} \tag{59}$$

are the integrity bases ($\{\cdot\}$ denotes the trace). Pope [19] only obtained the solution to (51) corresponding to the Launder, Reece and Rodi [20] model simplified to two-dimensional mean turbulent flows in an inertial frame – a case for which the calculations become much simpler since only the integrity bases $\mathbf{T}^{(1)} - \mathbf{T}^{(3)}$ are linearly independent. Gatski and Speziale [3] showed that the general solution (58) for three-dimensional turbulent flows is as follows:

$$\begin{aligned}
G^{(1)} &= -\tfrac{1}{2}(6 - 3\eta_1 - 21\eta_2 - 2\eta_3 + 30\eta_4)/D, & G^{(6)} &= -9/D \\
G^{(2)} &= -(3 + 3\eta_1 - 6\eta_2 + 2\eta_3 + 6\eta_4)/D, & G^{(7)} &= 9/D \\
G^{(3)} &= (6 - 3\eta_1 - 12\eta_2 - 2\eta_3 - 6\eta_4)/D, & G^{(8)} &= 9/D \\
G^{(4)} &= -3(3\eta_1 + 2\eta_3 + 6\eta_4)/D, & G^{(9)} &= 18/D \\
G^{(5)} &= -9/D, & G^{(10)} &= 0
\end{aligned} \tag{60}$$

$$D = 3 - \frac{7}{2}\eta_1 + \eta_1^2 - \frac{15}{2}\eta_2 - 8\eta_1\eta_2 + 3\eta_2^2 - \eta_3 + \frac{2}{3}\eta_1\eta_3$$

$$-2\eta_2\eta_3 + 21\eta_4 + 24\eta_5 + 2\eta_1\eta_4 - 6\eta_2\eta_4 \tag{61}$$

$$\eta_1 = \{\overline{\mathbf{S}}^{*2}\},\ \eta_2 = \{\overline{\mathbf{W}}^{*2}\},\ \eta_3 = \{\overline{\mathbf{S}}^{*3}\},$$
$$\eta_4 = \{\overline{\mathbf{S}}^{*}\overline{\mathbf{W}}^{*2}\},\ \eta_5 = \{\overline{\mathbf{S}}^{*2}\overline{\mathbf{W}}^{*2}\}. \tag{62}$$

While the results provided in (60) - (62) constitute the general solution of (51) for three-dimensional turbulent flows, questions can be raised about its overall usefulness. As alluded to earlier, (51) is based on the use of (48) which is only formally valid for *two-dimensional* mean turbulent flows that are near equilibrium. For two-dimensional mean turbulent flows, (60) - (62) simplifies substantially to the form

$$b^*_{ij} = -\frac{3}{3-2\eta^2+6\xi^2}\left[\overline{S}^*_{ij} + \overline{S}^*_{ik}\overline{W}^*_{kj} + \overline{S}^*_{jk}\overline{W}^*_{ki} - 2\left(\overline{S}^*_{ik}\overline{S}^*_{kj} - \frac{1}{3}\overline{S}^*_{kl}\overline{S}^*_{kl}\delta_{ij}\right)\right] \tag{63}$$

where

$$\eta \equiv (\overline{S}^*_{ij}\overline{S}^*_{ij})^{1/2}, \quad \xi = (\overline{W}^*_{ij}\overline{W}^*_{ij})^{1/2} \tag{64}$$

By making use of (52) - (55), we can write (63) in terms of the Reynolds stress tensor as follows:

$$\tau_{ij} = \frac{2}{3}K\delta_{ij} - \frac{3}{3-2\eta^2+6\xi^2}\left[\alpha_1\frac{K^2}{\varepsilon}\overline{S}_{ij} + \alpha_2\frac{K^3}{\varepsilon^2}(\overline{S}_{ik}\overline{W}_{kj} + \overline{S}_{jk}\overline{W}_{ki}) - \alpha_3\frac{K^3}{\varepsilon^2}\left(\overline{S}_{ik}\overline{S}_{kj} - \frac{1}{3}\overline{S}_{kl}\overline{S}_{kl}\delta_{ij}\right)\right] \tag{65}$$

where

$$\alpha_1 = g\left(\frac{4}{3} - C_2\right) \tag{66}$$

$$\alpha_2 = \frac{1}{2}g^2\left(\frac{4}{3} - C_2\right)(2 - C_4) \tag{67}$$

$$\alpha_3 = g^2\left(\frac{4}{3} - C_2\right)(2 - C_3) \tag{68}$$

The coefficients α_1, α_2 and α_3 are *not* constants but rather are related to the coefficients $C_1 - C_4$ and g. In mathematical terms, they are "projections" of the fixed points of $\mathcal{A}_{ij}$ and $\mathcal{M}_{ijkl}$ onto the fixed points of b_{ij}, which can vary from one flow to the next. *However, for 2-D turbulent flows, $C_1 - C_4$ can be approximated by constants due to the linear dependence on b_{ij} which allows us to use superposition.*

Gatski and Speziale [3] evaluated $C_1 - C_4$ using the SSG second-order closure which will be discussed later; this model was calibrated largely based on the use of data for homogeneous shear flow (see Table 1).

Equilibrium Values	LRR Model	SSG Model	Data
$(b_{11})_\infty$	0.158	0.204	0.201
$(b_{22})_\infty$	-0.123	-0.148	-0.147
$(b_{12})_\infty$	-0.187	-0.156	-0.150
$(SK/\epsilon)_\infty$	5.32	5.98	6.08

Table 1. Comparison of the predictions of the Launder, Reece and Rodi (LRR) model and the Speziale, Sarkar and Gatski (SSG) model with the experimental data of Tavoularis and Corrsin [18] for homogeneous turbulent shear flow.

The constant values that are taken for $C_1 - C_4$ are given by (see Gatski and Speziale [3]):

$$C_1 = 6.80,\ C_2 = 0.36,\ C_3 = 1.25,\ C_4 = 0.40 \tag{69}$$

It should be noted at this point that if (63) is applied to turbulent flows that are far from equilibrium, singularities can arise through the vanishing of the denominator containing η and ξ (it is straightforward to show that this cannot happen in equilibrium turbulent flows). Hence, this model needs to be regularized before it is applied to complex turbulent flows that are not in equilibrium. This can be accomplished via a Padé type approximation whereby

$$\frac{3}{3 - 2\eta^2 + 6\xi^2} \approx \frac{3(1+\eta^2)}{3 + \eta^2 + 6\xi^2\eta^2 + 6\xi^2} \tag{70}$$

(see Gatski and Speziale [3]). It is a simple matter to show that (70) constitutes an excellent approximation for turbulent flows that are near equilibrium and, unlike the original expression, is a bounded and non-negative function for *all* values of η and ξ.

The representation (63) constitutes an anisotropic eddy viscosity model of the general form

$$b_{ij} = a_{ijkl}\frac{\partial \overline{v}_k}{\partial x_l} \tag{71}$$

where the fourth rank tensor a_{ijkl} depends on the symmetric and antisymmetric parts of the mean velocity gradients. Quadratic models of this type have recently been obtained by Yoshizawa [21], Speziale [22] and Rubinstein and Barton [23] based on two-scale DIA, continuum mechanics and RNG based techniques, respectively (in regard to the latter, see Yakhot and Orszag [24]). Furthermore, it must be noted that while the traditional implicit algebraic stress models such as that due to Rodi [25] (which is of the general form (51)) have an explicit solution of the form (63), they are ill-behaved and can give rise to divergent solutions when applied to non-equilibrium turbulent flows. This explains why previous anisotropic corrections to eddy viscosity models have only had limited success:

(i) A quadratic expansion is not adequate; the coefficients should depend nonlinearly on rotational and irrotational strain rates.

(ii) Only the regularized explicit solution to algebraic stress models – which has just recently emerged – has the proper such dependence. Traditional algebraic stress models are ill-behaved and should not be applied to complex turbulent flows that are significantly out of equilibrium.

If we have a clear cut separation of scales where

$$\eta,\ \xi \ll 1$$

then (65) reduces to the eddy viscosity model

$$\tau_{ij} = \frac{2}{3} K \delta_{ij} - 2 C_\mu \frac{K^2}{\varepsilon} \overline{S}_{ij} \tag{72}$$

which forms the basis for the standard $K - \varepsilon$ model of Launder and Spalding [26]. However, in basic turbulent shear flows, we do not have a separation of scales: η and ξ are of order one. Nonetheless, there are some circumstances where (65) yields results that are comparable to (72). For example, in the logarithmic region of an equilibrium turbulent boundary layer, the explicit algebraic stress model (65) yields

$$\tau_{xy} = -C_\mu \frac{K^2}{\varepsilon} \frac{d\overline{u}}{dy} \tag{73}$$

for the shear stress, where

$$C_\mu \approx 0.094 \tag{74}$$

given that $\partial \overline{v}_i / \partial x_j = d\overline{u}/dy\ \delta_{i1}\delta_{j2}$. This is virtually identical to the standard $K - \varepsilon$ model which, for this case, yields (73) with $C_\mu = 0.09$. Of course, for more complex turbulent flows the models are substantially different; unlike the standard $K - \varepsilon$ model, the explicit algebraic stress model has a strain-dependent eddy viscosity and anisotropic eddy viscosity terms.

In order to achieve closure, a modeled transport equation for the turbulent dissipation rate ε is needed. For homogeneous turbulence, the exact transport equation (32) for the turbulent dissipation rate reduces to:

$$\begin{aligned} \dot{\varepsilon} \;=\; & -\varepsilon_{ij} \frac{\partial \overline{v}_i}{\partial x_j} - \varepsilon_{ij}^{(c)} \frac{\partial \overline{v}_i}{\partial x_j} - 2\nu \overline{\frac{\partial u_k}{\partial x_i} \frac{\partial u_k}{\partial x_j} \frac{\partial u_i}{\partial x_j}} \\ & -2\nu^2 \overline{\frac{\partial^2 u_i}{\partial x_j \partial x_k} \frac{\partial^2 u_i}{\partial x_j \partial x_k}} \end{aligned} \tag{75}$$

where ε_{ij} is the turbulent dissipation rate tensor defined in (26) and

$$\varepsilon_{ij}^{(c)} = 2\nu \overline{\frac{\partial u_k}{\partial x_i}\frac{\partial u_k}{\partial x_j}} \tag{76}$$

is the complementary dissipation rate tensor. If we introduce the anisotropy of dissipation tensors

$$d_{ij} = \frac{\varepsilon_{ij} - \frac{2}{3}\varepsilon\delta_{ij}}{2\varepsilon} \tag{77}$$

$$d_{ij}^{(c)} = \frac{\varepsilon_{ij}^{(c)} - \frac{2}{3}\varepsilon\delta_{ij}}{2\varepsilon} \tag{78}$$

(where $\varepsilon \equiv \frac{1}{2}\varepsilon_{ii} \equiv \frac{1}{2}\varepsilon_{ii}^{(c)}$), a simple closure can be developed for the production of dissipation terms in (75). Here, it is assumed that

$$d_{ij} = C_d\, b_{ij}, \quad d_{ij}^{(c)} = C_d^*\, b_{ij}, \tag{79}$$

which physically implies that the anisotropy of dissipation is proportional to the anisotropy of the Reynolds stresses due to the fact that the former follows from the latter as a result of the energy cascade from large to small scales. Results from Direct Numerical Simulations (DNS) of homogeneous shear flow (Rogers, Moin and Reynolds [27]) only provide justification for (79) as, at best, a low order approximation.

The third correlation on the right-hand-side of (75) can be written in the form

$$2\nu \overline{\frac{\partial u_k}{\partial x_i}\frac{\partial u_k}{\partial x_j}\frac{\partial u_i}{\partial x_j}} = -\frac{7}{3\sqrt{15}} S_K R_t^{1/2} \frac{\varepsilon^2}{K} \tag{80}$$

where

$$S_K = -\frac{6\sqrt{15}}{7} \frac{\overline{\frac{\partial u_k}{\partial x_i}\frac{\partial u_k}{\partial x_j}\frac{\partial u_i}{\partial x_j}}}{\left(\overline{\frac{\partial u_m}{\partial x_n}\frac{\partial u_m}{\partial x_n}}\right)^{3/2}} \tag{81}$$

is the generalized velocity derivative skewness and $R_t \equiv K^2/\nu\varepsilon$ is the turbulence Reynolds number. For isotropic turbulence, (81) reduces to the classical definition of the velocity derivative skewness which is given by $S_K = -\overline{(\partial u/\partial x)^3}/[\overline{(\partial u/\partial x)^2}]^{3/2}$ (here we define the skewness with the negative gauge). In spectral space, the destruction of dissipation term on the right-hand-side of (75) behaves as follows:

$$2\nu^2 \overline{\frac{\partial^2 u_i}{\partial x_j \partial x_k}\frac{\partial^2 u_i}{\partial x_j \partial x_k}} \sim 2\nu^2 \int_0^\infty k^4 E(k,t) dk \tag{82}$$

where $E(k,t)$ is the three-dimensional energy spectrum. Consequently, most of the contributions to this term occur at high wavenumbers where the energy spectrum scales with the Kolmogorov length scale, $l_k \equiv \nu^{3/4}/\varepsilon^{1/4}$. With this Kolmogorov scaling, it follows that

$$2\nu^2 \overline{\frac{\partial^2 u_i}{\partial x_j \partial x_k}\frac{\partial^2 u_i}{\partial x_j \partial x_k}} = \frac{7}{3\sqrt{15}} G_K R_t^{1/2} \frac{\varepsilon^2}{K} + C_{\varepsilon 2}\frac{\varepsilon^2}{K} \tag{83}$$

(see Speziale and Bernard [28]). The direct substitution of (79), (80) and (83) into (75) yields the transport equation

$$\dot{\varepsilon} = -C_{\varepsilon 1}\frac{\varepsilon}{K}\tau_{ij}\frac{\partial \overline{v}_i}{\partial x_j} + \frac{7}{3\sqrt{15}}(S_K - G_K)R_t^{1/2}\frac{\varepsilon^2}{K} - C_{\varepsilon 2}\frac{\varepsilon^2}{K} \tag{84}$$

where $C_{\varepsilon 1} = C_d + C_d^*$ (in general homogeneous turbulence, $C_{\varepsilon 1}$, $C_{\varepsilon 2}$, S_K, and G_K can be functions of time). For equilibrium turbulent flows at high Reynolds numbers,

$$S_K = G_K \tag{85}$$

and $C_{\varepsilon 1}$ and $C_{\varepsilon 2}$ can be approximated as constants (when (85) is not valid, then ε changes on the Kolmogorov time scale – an extremely rapid change at high Reynolds numbers that constitutes a non-equilibrium flow situation). This leads us to the commonly used modeled dissipation rate equation for homogeneous turbulence:

$$\dot{\varepsilon} = -C_{\varepsilon 1}\frac{\varepsilon}{K}\tau_{ij}\frac{\partial \overline{v}_i}{\partial x_j} - C_{\varepsilon 2}\frac{\varepsilon^2}{K} \tag{86}$$

with $C_{\varepsilon 1}$ and $C_{\varepsilon 2}$ taken to be constants. Typically, $C_{\varepsilon 2}$ is determined from the decay of isotropic turbulence; for isotropic decay, (86) implies that (cf. Speziale [1])

$$K \sim t^{-\frac{1}{(C_{\varepsilon 2}-1)}}. \tag{87}$$

The most cited experimental data [29] indicates that the exponent of the decay law (87) has a mean value of approximately 1.2; this implies a value for $C_{\varepsilon 2} \approx 1.83$. In practice, a value of $C_{\varepsilon 2} = 1.90$ has been more commonly used starting with Launder, Reece and Rodi [20]. This typically has been used with a value of $C_{\varepsilon 1} = 1.44$ based on a calibration with a range of benchmark turbulent shear flows.

Recently, Speziale and Gatski [30] showed that when the effects of anisotropic dissipation are more rigorously accounted for, a variable $C_{\varepsilon 1}$ results that is of the form $C_{\varepsilon 1} = C_{\varepsilon 1}(\eta, \xi)$. This form is obtained by starting with a modeled transport equation for the full tensor dissipation ε_{ij}. An algebraic equation – analogous to that obtained from the ASM approximation for the Reynolds stress – is arrived at when the standard equilibrium hypothesis

$$\dot{d}_{ij} = 0$$

is invoked. For two-dimensional mean turbulent flows, it has the exact form:

$$
\begin{aligned}
d_{ij} &= -2C_{\mu\epsilon}\left[\overline{S}^*_{ij} + \left(\frac{\frac{7}{11}\alpha_3 + \frac{1}{11}}{C_{\epsilon 5} + \mathcal{P}/\varepsilon - 1}\right)\right. \\
&\quad \times(\overline{S}^*_{ik}\overline{\omega}^*_{jk} + \overline{S}^*_{jk}\overline{\omega}^*_{ik}) \\
&\quad + \left(\frac{\frac{30}{11}\alpha_3 - \frac{2}{11}}{C_{\epsilon 5} + \mathcal{P}/\varepsilon - 1}\right)\left(\overline{S}^*_{ik}\overline{S}^*_{jk}\right. \\
&\quad \left.\left. -\frac{1}{3}\overline{S}^*_{mn}\overline{S}^*_{mn}\delta_{ij}\right)\right]
\end{aligned}
\tag{88}
$$

where

$$
\begin{aligned}
C_{\mu\epsilon} &= \frac{1}{15(C_{\epsilon 5} + \mathcal{P}/\varepsilon - 1)}\left[1\right. \\
&\quad +2\overline{\omega}^*_{ij}\overline{\omega}^*_{ij}\left(\frac{\frac{7}{11}\alpha_3 + \frac{1}{11}}{C_{\epsilon 5} + \mathcal{P}/\varepsilon - 1}\right)^2 \\
&\quad \left. -\frac{2}{3}\left(\frac{\frac{15}{11}\alpha_3 - \frac{1}{11}}{C_{\epsilon 5} + \mathcal{P}/\varepsilon - 1}\right)\overline{S}^*_{ij}\overline{S}^*_{ij}\right]^{-1}
\end{aligned}
$$

$$
\overline{S}^*_{ij} = \overline{S}_{ij}\frac{K}{\varepsilon}, \quad \overline{\omega}^*_{ij} = \overline{\omega}_{ij}\frac{K}{\varepsilon}
$$

and $C_{\epsilon 5}$ and α_3 are constants (Speziale and Gatski [30]). The substitution of these algebraic equations into the contraction of the ε_{ij} transport equation yields the scalar dissipation rate equation (86) with

$$
C_{\varepsilon 1} = 1 + \frac{2}{15C_\mu}\left[\frac{(1+\alpha)(C_{\epsilon 5} + C_\mu\eta^2 - 1)}{(C_{\epsilon 5} + C_\mu\eta^2 - 1)^2 + \beta_1^2\xi^2 - \frac{1}{3}\beta_2^2\eta^2}\right] \tag{89}
$$

where

$$
\eta = (2\overline{S}^*_{ij}\overline{S}^*_{ij})^{1/2}, \quad \xi = (2\overline{\omega}^*_{ij}\overline{\omega}^*_{ij})^{1/2}
$$

$$
\alpha = \frac{3}{4}\left(\frac{14}{11}\alpha_3 - \frac{16}{33}\right), \quad \beta_1 = \frac{7}{11}\alpha_3 + \frac{1}{11}
$$

$$
\beta_2 = \frac{15}{11}\alpha_3 - \frac{1}{11}, \quad C_{\epsilon 5} \approx 5, \quad \alpha_3 \approx 0.6.
$$

The constants α_3 and $C_{\epsilon 5}$ were evaluated using DNS results for homogeneous shear flow (Rogers, Moin and Reynolds [27]).

For two-dimensional turbulent shear flows that are in equilibrium, (89) yields

$$
C_{\varepsilon 1} \approx 1.4
$$

which is remarkably close to the traditionally chosen constant value of $C_{\varepsilon 1} = 1.44$. It is interesting to note that an alternative variable $C_{\varepsilon 1}$ of the form $C_{\varepsilon 1} = C_{\varepsilon 1}(\eta)$ was recently proposed by Yakhot *et al.* [31] based on a heuristic Padé approximation. However, the model of Speziale and Gatski [30] depends on rotational as well as irrotational strain rates (η, ξ). It has long been recognized that the dissipation rate is dramatically altered by rotations. The results of Speziale and Gatski [30] clearly show that this effect can be rationally incorporated by accounting for anisotropic dissipation. To the best knowledge of the author, this model constitutes the first systematic introduction of rotational effects into the scalar dissipation rate equation. Previous attempts to account for this effect (see Raj [32]; Hanjalic and Launder [33]; and Bardina, Ferziger and Rogallo [34]) were largely *ad hoc*.

For *weakly* inhomogeneous turbulent flows that are near equilibrium, we can extend the K and ε transport equations by the addition of turbulent diffusion terms that are obtained by a formal expansion technique:

$$\frac{\partial K}{\partial t} + \overline{\mathbf{v}} \cdot \nabla K = \mathcal{P} - \varepsilon + \frac{\partial}{\partial x_i}\left(\frac{\nu_T}{\sigma_k}\frac{\partial K}{\partial x_i}\right) + \nu \nabla^2 K \tag{90}$$

$$\frac{\partial \varepsilon}{\partial t} + \overline{\mathbf{v}} \cdot \nabla \varepsilon = C_{\varepsilon 1}\frac{\varepsilon}{K}\mathcal{P} - C_{\varepsilon 2}\frac{\varepsilon^2}{K} + \frac{\partial}{\partial x_i}\left(\frac{\nu_T}{\sigma_\varepsilon}\frac{\partial \varepsilon}{\partial x_i}\right) + \nu \nabla^2 \varepsilon \tag{91}$$

where σ_k and σ_ε are constants that typically assume the values of 1.0 and 1.3, respectively.

This model can be integrated directly to a solid boundary, where the no-slip condition is applied, without the need for *ad hoc* wall damping functions. It is only necessary to remove the singularity in the destruction of dissipation term

$$-C_{\varepsilon 2}\frac{\varepsilon^2}{K}$$

on the right-hand-side of (91). Durbin [35] argued that this expression should be replaced with the term

$$-C_{\varepsilon 2}\frac{\varepsilon}{T}$$

where T is the turbulent time scale. For high Reynolds number turbulence, $T = K/\varepsilon$; for low Reynolds number turbulence near a wall, the turbulent time scale is proportional to the Kolmogorov time scale, i.e., $T \propto \sqrt{\nu/\varepsilon}$. These considerations lead Durbin [35] to propose the expression

$$T = \max\left[\frac{K}{\varepsilon}, C_K\sqrt{\nu/\varepsilon}\right]$$

where C_K is a constant of order one. A damping function, however, can also be used. Namely, we can take the destruction term to be

$$-C_{\varepsilon 2} f_2 \frac{\varepsilon^2}{K}$$

where f_2 is a wall damping function which, for example, can be chosen to be of the form

$$f_2 = 1 - \exp(-R_y/10)$$

where $R_y \equiv K^{1/2}y/\nu$ is the turbulence Reynolds number based on the distance y from the wall. No wall damping is needed in the eddy viscosity; the strain-dependent terms in the eddy viscosity provide natural damping as the wall is approached (see Speziale and Abid [36]).

We will now consider several non-trivial applications of the two-equation model discussed herein which can be referred to as an explicit algebraic stress model (ASM) based on the SSG second-order closure. The first case that will be considered is homogeneous shear flow in a rotating frame (see Figure 1). In this flow, an initially isotropic turbulence (with turbulent kinetic energy K_0 and turbulent dissipation rate ε_0) is suddenly subjected to a uniform shear with constant shear rate S in a reference frame rotating steadily with angular velocity Ω. In Figures 2(a)-2(c), the time evolution of the turbulent kinetic energy predicted by this new two-equation model is compared with the large-eddy simulations (LES) of Bardina, Ferziger and Reynolds [37], as well as with the predictions of the standard $K - \varepsilon$ model and the full SSG second-order closure. From these results, it is clear that the new two-equation model yields the correct growth rate for pure shear flow ($\Omega/S = 0$) and properly responds to the stabilizing effect of the rotations $\Omega/S = 0.5$ and $\Omega/S = -0.5$. These results are remarkably close to those obtained from the full SSG second-order closure as shown in Figure 2. In contrast to these results, the standard $K - \varepsilon$ model overpredicts the growth rate of the turbulent kinetic energy in pure shear flow ($\Omega/S = 0$) and fails to predict the stabilizing effect of the rotations illustrated in Figures 2(b)-2(c). Since the standard $K - \varepsilon$ model makes use of the Boussinesq eddy viscosity hypothesis, it is oblivious to the application of a system rotation (i.e., it yields the *same* solution for all values of Ω/S). The new two-equation model predicts unstable flow only for the intermediate band of rotation rates $-0.09 \leq \Omega/S \leq 0.53$; this is generally consistent with linear stability theory that predicts unstable flow for $0 \leq \Omega/S \leq 0.5$.

In Figure 3, the prediction of this new two-equation model for the mean velocity profile in rotating channel flow is compared with the experimental data of Johnston, Halleen and Lezius [38] for a rotation number $Ro = 0.068$. It is clear from these results that the model correctly predicts that the mean velocity profile is *asymmetric* in line with the experimental data – an effect that arises from Coriolis forces. In contrast to these results, the standard $K-\varepsilon$ model incorrectly predicts a symmetric mean velocity profile identical to that obtained in an inertial frame (the standard $K-\varepsilon$ model is oblivious to rotations of the reference frame, as alluded to above). As demonstrated by Gatski and Speziale [3], the results obtained in

Figure 3 with this new two-equation model are virtually as good as those obtained from a full second-order closure. This is due to the fact that a representation is used for the Reynolds stress tensor that is formally derived from a second-order closure (the SSG model) in the equilibrium limit. It is now clear that previous claims that two-equation models cannot systematically account for rotational effects were erroneous.

Two examples will now be presented that illustrate the enhanced predictions that are obtained for turbulent flows exhibiting effects arising from normal Reynolds stress differences. Here, we will show results obtained from the nonlinear $K-\varepsilon$ model of Speziale [22]. For turbulent shear flows that are predominantly unidirectional, with secondary flows or recirculation zones driven by small normal Reynolds stress differences, a quadratic approximation of the anisotropic eddy viscosity model discussed herein collapses to the nonlinear $K-\varepsilon$ model (see Gatski and Speziale [3]). In Figure 4, it is demonstrated that the nonlinear $K-\varepsilon$ model predicts an eight-vortex secondary flow, in a square duct, in line with experimental observations; on the other hand, the standard $K-\varepsilon$ model erroneously predicts that there is no secondary flow. In order to be able to predict secondary flows in non-circular ducts, the axial mean velocity $\overline{v}_z$ must give rise to a non-zero normal Reynolds stress difference $\tau_{yy}-\tau_{xx}$ (see Speziale and Ngo [39]). This requires an *anisotropic* eddy viscosity (any isotropic eddy viscosity, including that used in the standard $K-\varepsilon$ model, yields a vanishing normal Reynolds stress difference which makes it impossible to describe these secondary flows).

In Figure 5, results obtained from the nonlinear $K-\varepsilon$ model are compared with the experimental data of Kim, Kline and Johnston [40] and Eaton and Johnston [41] for turbulent flow past a backward facing step. It is clear that these results are excellent: reattachment is predicted at $x/H \approx 7.0$ in close agreement with the experimental data. In contrast to these results, the standard $K-\varepsilon$ model predicts reattachment at $x/H \approx 6.25$ – an 11% underprediction. This error predominantly results from the inaccurate prediction of normal Reynolds stress anisotropies in the recirculation zone as discussed by Speziale and Ngo [39]. As alluded to above, the new two-equation model can be integrated directly to a solid boundary with no wall damping. In Figure 6, the skin friction coefficient obtained from this model – plotted as function of the Reynolds number based on the momentum thickness, R_θ – is compared with experimental data and with results obtained from the $K-\varepsilon$ model with wall damping. Clearly, the results are extremely good.

6. Second-Order Closure Models

These more complex closures are based on the full Reynolds stress transport equation with turbulent diffusion:

$$\frac{\partial \tau_{ij}}{\partial t} + \overline{v}_k \frac{\partial \tau_{ij}}{\partial x_k} = -\tau_{ik}\frac{\partial \overline{v}_j}{\partial x_k} - \tau_{jk}\frac{\partial \overline{v}_i}{\partial x_k} + \Phi_{ij}$$

$$-{}_D\varepsilon_{ij} - \frac{2}{3}\varepsilon\delta_{ij} - \frac{\partial C_{ijk}}{\partial x_k} + \nu\nabla^2\tau_{ij} \tag{92}$$

where ${}_D\varepsilon_{ij}$ is the deviatoric part of the dissipation rate tensor. Full second-order closure models are needed for turbulent flows with:

(i) Relaxation effects;

(ii) Nonlocal effects arising from turbulent diffusion that can give rise to counter-gradient transport.

In virtually all existing full second-order closures for inhomogeneous turbulent flows, Φ_{ij} and ${}_D\varepsilon_{ij}$ are modeled by their homogeneous forms. The pressure-strain correlation Φ_{ij} is modeled as

$$\Phi_{ij} = \varepsilon\mathcal{A}_{ij}(\mathbf{b}) + K\mathcal{M}_{ijkl}(\mathbf{b})\frac{\partial \overline{v}_k}{\partial x_l} \tag{93}$$

as discussed earlier. In Section 5, the equilibrium limit of the Speziale, Sarkar and Gatski (SSG) model was provided. For turbulent flows where there are departures from equilibrium, the SSG model takes the form (see Speziale, Sarkar and Gatski [2])

$$\begin{aligned}\Phi_{ij} \;=\; & -(C_1\varepsilon + C_1^*\mathcal{P})b_{ij} + C_2\varepsilon\,(b_{ik}b_{kj} \\ & -\frac{1}{3}b_{kl}b_{kl}\delta_{ij}) + (C_3 - C_3^* II_b^{1/2})K\overline{S}_{ij} \\ & +C_4K(b_{ik}\overline{S}_{jk} + b_{jk}\overline{S}_{ik} - \frac{2}{3}b_{kl}\overline{S}_{kl}\delta_{ij}) \\ & +C_5K(b_{ik}\overline{W}_{jk} + b_{jk}\overline{W}_{ik})\end{aligned} \tag{94}$$

where

$$C_1 = 3.4,\ C_1^* = 1.80,\ C_2 = 4.2,\ C_3 = \frac{4}{5}$$
$$C_3^* = 1.30,\ C_4 = 1.25,\ C_5 = 0.40,\ II_b = b_{ij}b_{ij}.$$

The Launder, Reece and Rodi [20] model is recovered as a special case of the SSG model if we set

$$C_1 = 3.0,\ C_1^* = 0,\ C_2 = 0,\ C_3 = \frac{4}{5},\ C_3^* = 0,$$

$$C_4 = 1.75,\ C_5 = 1.31.$$

In most applications, at high Reynolds numbers, the Kolmogorov assumption of local isotropy is typically invoked where

$$_D\varepsilon_{ij} = 0$$

(then, $\varepsilon_{ij} = \frac{2}{3}\varepsilon\delta_{ij}$ and a modeled transport equation for the scalar dissipation rate ε is solved that is of the same general form as that discussed in Section 5). However, this assumption is debatable as discussed by Durbin and Speziale [42]. More generally, a representation of the form

$$_D\varepsilon_{ij} = 2\varepsilon d_{ij}$$

can be used where the algebraic model (88) of Speziale and Gatski [30], discussed in Section 5, is implemented.

The only additional model that is needed for closure in high-Reynolds-number inhomogeneous turbulent flows is a model for the third-order diffusion correlation C_{ijk}. This is typically modeled using a gradient transport hypothesis:

$$C_{ijk} = \mathcal{D}_{ijklmn}\frac{\partial \tau_{lm}}{\partial x_n}. \tag{95}$$

Some examples of commonly used models are as follows: *Launder, Reece and Rodi [20] Model*

$$C_{ijk} = -C_s\frac{K}{\varepsilon}\left(\tau_{im}\frac{\partial \tau_{jk}}{\partial x_m} + \tau_{jm}\frac{\partial \tau_{ik}}{\partial x_m} + \tau_{km}\frac{\partial \tau_{ij}}{\partial x_m}\right) \tag{96}$$

Mellor and Herring [43] Model

$$C_{ijk} = -\frac{2}{3}C_s\frac{K^2}{\varepsilon}\left(\frac{\partial \tau_{jk}}{\partial x_i} + \frac{\partial \tau_{ik}}{\partial x_j} + \frac{\partial \tau_{ij}}{\partial x_k}\right) \tag{97}$$

Daly and Harlow [44] Model

$$C_{ijk} = -2C_s\frac{K}{\varepsilon}\tau_{kl}\frac{\partial \tau_{ij}}{\partial x_l} \tag{98}$$

where $C_s \approx 0.11$ is a constant. When these models are used in a full second-order closure, counter-gradient transport effects can be described.

There is no question that, in principle, second-order closures account for more physics. This is quite apparent for turbulent flows exhibiting relaxation effects. The return to isotropy problem is a prime example where suddenly, at time $t = 0$, the mean strains in a homogeneous turbulence are shut off; the flow then gradually returns to isotropy (i.e., $b_{ij} \to 0$ as $t \to \infty$). In Figure 7, results for the Reynolds stress anisotropy tensor obtained from the Speziale,

Sarkar and Gatski (SSG) and Launder, Reece and Rodi (LRR) models are compared with the experimental data of Choi and Lumley [45] for the return-to-isotropy from plane strain (here, $\tau = \varepsilon_0 t/K_0$). It is clear from these results that the models predict a gradual return to isotropy in line with the experimental data. In contrast to these results, all two-equation models – including the more sophisticated one based on an anisotropic eddy viscosity derived herein – erroneously predict that at $\tau = 0$, b_{ij} abruptly goes to zero. In addition, it is worth noting that while the SSG model was derived and calibrated based on near equilibrium two-dimensional mean turbulent flows, it performs remarkably well on certain three-dimensional, homogeneously strained turbulent flows. The predictions of the SSG and LRR models for the normal Reynolds stress anisotropies, compared in Figure 8 with the direct simulations of Lee and Reynolds [46] for the axisymmetric expansion, demonstrate this point (here, $t^* = \Gamma t$ where Γ is the strain rate).

While the previous results are encouraging, it must be noted that the *Achilles heel of second-order closures is wall-bounded turbulent flows*:

(i) Ad hoc wall reflection terms are needed in most pressure-strain models (that depend inversely on the distance y from the wall) in order to mask deficient predictions for the logarithmic region of a turbulent boundary layer;

(ii) Near-wall models must typically be introduced that depend on the unit normal to the wall – a feature that makes it virtually impossible to systematically integrate second-order closures in complex geometries (see So *et al.* [47]).

In regard to the first point, it is rather shocking as to what the level of error is in many existing second-order closures for the logarithmic region of an equilibrium turbulent boundary layer, when no ad hoc wall reflection terms are used. This can be seen in Table 2 where the predictions of the Launder, Reece and Rodi (LRR), Shih and Lumley (SL), Fu, Launder and Tselepidakis (FLT) and SSG models are compared with experimental data (Laufer [48]) for the log-layer of turbulent channel flow. Most of the models yield errors ranging from 30% to 100%. These models are then typically forced into agreement with the experimental data by the addition of ad hoc wall reflection terms that depend inversely on the distance from the wall – an alteration that compromises the ability to apply a model in complex geometries where the wall distance is not always uniquely defined. Only the SSG model yields acceptable results for the log-layer without a wall reflection term. This results from two factors: (a) a careful and accurate calibration of homogeneous shear flow (see Table 3) and (b) the use of a Rotta coefficient $\frac{1}{2}C_1$ that is not too far removed from one (see Abid and Speziale [49]). The significance of these results is demonstrated in Figure 9 where full Reynolds stress computations of turbulent channel flow are compared with the experimental

data of Laufer [48]. It is clear that the same trends are exhibited in these results as with those shown in Table 2 which were obtained by a simplified log-layer analysis.

The near-wall problem largely arises from the use of homogeneous pressure-strain models of the form (93) that are only theoretically justified for near-equilibrium homogeneous turbulence. Recently, Durbin [35] developed an elliptic relaxation model that accounts for wall blocking – and introduces nonlocal effects in the vicinity of walls – eliminating the need for ad hoc wall damping functions. While this is a promising new approach, it does not alleviate the problems that the commonly used pressure-strain models have in non-equilibrium homogeneous turbulence (the Durbin [35] model collapses to the standard hierarchy of pressure-strain models given above in the limit of homogeneous turbulence). The failure of these models in non-equilibrium homogeneous turbulence can be illustrated by the example shown in Figure 10. This constitutes a rapidly distorted homogeneous shear flow that, initially, is far from equilibrium since $SK_0/\varepsilon_0 = 50$ (the equilibrium value of SK/ε is approximately 5). It is apparent from these

CHANNEL FLOW

Equilibrium Values	LRR Model	SL Model	FLT Model	SSG Model	Experimental Data
b_{11}	0.129	0.079	0.141	0.201	0.22
b_{12}	-0.178	-0.116	-0.162	-0.160	-0.16
b_{22}	-0.101	-0.082	-0.099	-0.127	-0.15
b_{33}	-0.028	0.003	-0.042	-0.074	-0.07
SK/ε	2.80	4.30	3.09	3.12	3.1

Table 2. Comparison of the model predictions for the equilibrium values in the log-layer ($\mathcal{P}/\varepsilon = 1$) with the experimental data of Laufer [48] for channel flow.

HOMOGENEOUS SHEAR FLOW

Equilibrium Values	LRR Model	SL Model	FLT Model	SSG Model	Experimental Data
b_{11}	0.152	0.120	0.196	0.218	0.21
b_{12}	-0.186	-0.121	-0.151	-0.164	-0.16
b_{22}	-0.119	-0.122	-0.136	-0.145	-0.14
b_{33}	-0.033	0.002	-0.060	-0.073	-0.07
SK/ε	4.83	7.44	5.95	5.50	5.0

Table 3. Comparison of the model predictions for the equilibrium values in homogeneous shear flow ($\mathcal{P}/\varepsilon = 1.8$) with the experimental data of Tavoularis and Karnik [50].

results that all of the models perform poorly relative to the DNS of Lee *et al.* [51]. Even the SSG model, which does extremely well for homogeneous shear flow that is not far from equilibrium, dramatically overpredicts the growth rate of the turbulent kinetic energy for this strongly non-equilibrium test case.

In the opinion of the author, it is a vacuous exercise to develop more complex models of the form (93) using non-equilibrium constraints such as *Material Frame-Indifference (MFI) in the two-dimensional limit* (Speziale [52, 53]) or *realizability* (Schumann [54] and Lumley [16]). While these constraints are a rigorous consequence of the Navier-Stokes equations, they typically deal with flow situations that are far from equilibrium (two-dimensional turbulence and one or two-component turbulence) where (93) would not be expected to apply in the first place. Ristorcelli, Lumley and Abid [55] – following the earlier work by Haworth and Pope [56] and Speziale [57, 58] – developed a pressure-strain model of the form (93) that satisfies MFI in the 2-D limit. Shih and Lumley [59] attempted to develop models of the form (93) that satisfy the strong form of realizability of Schumann [54]. Reynolds [17] has attempted to develop models of this form which are consistent with Rapid Distortion Theory (RDT). All of these models involve complicated expressions for M_{ijkl} that are *nonlinear* in b_{ij}. From its definition, M_{ijkl} is linear in the energy spectrum tensor $E_{kl}(\mathbf{k},t)$ (see Eq. (47)). Since,

$$b_{ij} = \frac{\tau_{ij} - \frac{2}{3}K\delta_{ij}}{2K}$$

where τ_{ij} is given by (45), it follows that models for M_{ijkl} that are nonlinear in b_{ij} are also nonlinear in E_{ij}. This is a *fundamental inconsistency* that dooms these models to failure. It is clear that is impossible to describe a range of RDT flows – which are linear – with nonlinear models (the principle of superposition is violated). Furthermore, Shih and Lumley [59, 60] unnecessarily introduce higher degree nonlinearities and non-analyticity to satisfy realizability. In the process of doing so, they arrive at a model that is neither realizable nor capable of describing even basic turbulent flows (see Speziale, Abid and Durbin [61], Durbin and Speziale [62] and Speziale and Gatski [63]).

Entirely new non-equilibrium models are needed for the pressure-strain correlation and the dissipation rate tensor. The former should contain nonlinear strain rate effects and the latter should account for the effects of anisotropic dissipation and non-equilibrium vortex stretching where $S_K \neq G_K$ in (84) (see Bernard and Speziale [64] and Speziale and Bernard [28]). Models of this type are currently under investigation for the Office of Naval Research *ARI on Nonequilibrium Turbulence.*

7. Conclusion

The following conclusions and recommendations for Naval Hydrodynamics applications can now be made:

(1) For turbulent flows with complex wall bounded or free surface geometries, two-equation models with an anisotropic eddy viscosity – that are integrated directly to a solid boundary with the no slip condition applied – should be used for the immediate future. A new generation of two-equation models, systematically derived from second-order closures, has emerged that is far superior to the commonly used $K - \varepsilon$ model and competitive with existing full second-order closures.

(2) There is no question that full second-order closure models do, in principle, account for more turbulence physics than two-equation models. However, current versions of these models have major problems when integrated directly to a solid boundary with the no-slip condition applied. They also perform poorly in even simple turbulent flows that are far from equilibrium. Until these problems are overcome, their use should be limited to free turbulent shear flows that are diffusion dominated or to wall bounded turbulent shear flows which exhibit complex turbulence physics that does not preclude the use of simple law of the wall boundary conditions.

Research is currently underway, as part of the Office of Naval Research *ARI on Nonequilibrium Turbulence*, to extend these models to turbulent flows that are far from equilibrium and to resolve the near-wall problem. With the incorporation of improvements along these lines, we should start to see Reynolds stress models make a major impact on the computation of the turbulent flows of relevance to Naval Hydrodynamics applications.

References

1. Speziale, C. G., "Analytical methods for the development of Reynolds stress closures in turbulence," *Ann. Rev. Fluid Mech.*, Vol. 23, 1991, pp. 107-157.

2. Speziale, C. G., Sarkar, S. and Gatski, T. B., "Modeling the pressure-strain correlation of turbulence: An invariant dynamical systems approach," *J. Fluid Mech.*, Vol. 227, 1991, pp. 245-272.

3. Gatski, T. B. and Speziale, C. G., "On explicit algebraic stress models for complex turbulent flows," *J. Fluid Mech.*, Vol. 254, 1993, pp. 59-78.

4. Hinze, J. O., *Turbulence*, 2nd ed., McGraw-Hill, New York, 1975.

5. Lumley, J. L., "Toward a turbulent constitutive equation," *J. Fluid Mech.*, Vol. 41, 1970, pp. 413-434.

6. Prandtl, L., "Über die ausgebildete turbulenz," *ZAMM*, Vol. 5, 1925, pp. 136-139.

7. Smagorinsky, J., "General circulation experiments with the primitive equations," *Mon. Weather Review*, Vol. 91, 1963, pp. 99-165.

8. Cebeci, T. and Smith, A. M. O., *Analysis of Turbulent Boundary Layers*, Academic Press, New York, 1974.

9. Baldwin, B. S. and Lomax, H., "Thin-layer approximation and algebraic model for separated turbulent flows," *AIAA Paper No. 78-257*, 1978.

10. Prandtl, L., "Über ein neues formelsystem für die ausgebildete turbulenz," *Nachr. Akad. Wiss. Göttingen Math. Phys. Kl*, Vol. 6, 1945, pp. 6-19.

11. Kolmogorov, A. N., "The equations of turbulent motion in an incompressible fluid," *Isv. Acad. Sci. USSR, Phys.*, Vol. 6, 1942, pp. 56-58.

12. Norris, L. H. and Reynolds, W. C., "Turbulent channel flow with a moving wavy boundary," *Stanford University Technical Report FM-10*, 1975.

13. Rodi, W., Mansour, N. N. and Michelassi, V., "One-equation near-wall turbulence modeling with the aid of direct simulation data," *ASME J. Fluids Eng.*, Vol. 115, 1993, pp. 196-205.

14. Baldwin, B. S. and Barth, T. J., "A one-equation turbulence transport model for high Reynolds number wall-bounded flows," *NASA TM-102847*, 1990.

15. Spalart, P. R. and Allmaras, S. R., "A one-equation turbulence model for aerodynamic flows," *AIAA Paper No. 92-439*, 1992.

16. Lumley, J. L., "Computational modeling of turbulent flows," *Adv. Appl. Mech.*, Vol. 18, 1978, pp. 123-176.

17. Reynolds, W. C., "Fundamentals of turbulence for turbulence modeling and simulation," in *Lecture Notes for Von Kármán Institute, AGARD Lect. Ser. No.* 86, 1987, pp. 1-66, NATO, New York.

18. Tavoularis, S. and Corrsin, S., "Experiments in nearly homogeneous turbulent shear flow with a uniform mean temperature gradient. Part I," *J. Fluid Mech.*, Vol. 104, 1981, pp. 311-347.

19. Pope, S. B., "A more general effective viscosity hypothesis," *J. Fluid Mech.*, Vol. 72, 1975, pp. 331-340.

20. Launder, B. E., Reece, G. J. and Rodi, W., "Progress in the development of a Reynolds stress turbulence closure," *J. Fluid Mech.*, Vol. 68, 1975, pp. 537-566.

21. Yoshizawa, A., "Statistical analysis of the deviation of the Reynolds stress from its eddy viscosity representation," *Phys. Fluids*, Vol. 27, 1984, pp. 1377-1387.

22. Speziale, C. G., "On nonlinear $K-\ell$ and $K-\varepsilon$ models of turbulence," *J. Fluid Mech.*, Vol. 178, 1987, pp. 459-475.

23. Rubinstein, R. and Barton, J. M., "Nonlinear Reynolds stress models and the renormalization group," *Phys. Fluids A*, Vol. 2, 1990, pp. 1472-1476.

24. Yakhot, V. and Orszag, S. A., "Renormalization group analysis of turbulence I. Basic theory," *J. Sci. Comp.*, Vol. 1, 1986, pp. 3-51.

25. Rodi, W., "A new algebraic relation for calculating the Reynolds stresses," *ZAMM*, Vol 56, 1976, pp. T219-221.

26. Launder, B. E. and Spalding, D. B., "The numerical computation of turbulent flows," *Comput. Methods Appl. Mech. Eng.*, Vol. 3, 1974, pp. 269-289.

27. Rogers, M. M., Moin, P. and Reynolds, W. C., "The structure and modeling of the hydrodynamic and passive scalar fields in homogeneous turbulent shear flow," *Stanford University Technical Report No. TF-25*, 1986.

28. Speziale, C. G. and Bernard, P. S., "The energy decay in self-preserving isotropic turbulence revisited," *J. Fluid Mech.*, Vol. 241, 1992, pp. 645-667.

29. Comte-Bellot, G. and Corrsin, S., "Simple Eulerian time correlation of full- and narrow-band velocity signals in grid-generated isotropic turbulence," *J. Fluid Mech.*, Vol. 48, 1971, pp. 273-337.

30. Speziale, C. G. and Gatski, T. B., "Modeling anisotropies in the dissipation rate of turbulence," *Bull. Am. Phys. Soc.*, Vol. 37, 1992, p. 1799.

31. Yakhot, V., Orszag, S. A., Thangam, S., Gatski, T. B. and Speziale, C. G., "Development of turbulence models for shear flows by a double expansion technique," *Phys. Fluids A*, Vol. 4,1992, pp. 1510-1520.

32. Raj, R., "Form of the turbulence dissipation equation as applied to curved and rotating turbulent flows," *Phys. Fluids*, Vol. 18, 1975, pp. 1241-1244.

33. Hanjalic, K. and Launder, B. E., "Sensitizing the dissipation equation to irrotational strains," *ASME J. Fluids Eng.*, Vol. 102, 1980, pp. 34-40.

34. Bardina, J., Ferziger, J. H. and Rogallo, R. S., "Effect of rotation on isotropic turbulence: Computation and modeling," *J. Fluid Mech.*, Vol. 154, 1985, pp. 321-336.

35. Durbin, P. A., "A Reynolds stress model for near-wall turbulence," *J. Fluid Mech.*, Vol. 249, 1993, pp. 465-498.

36. Speziale, C. G. and Abid, R., "A new near-wall model for Reynolds stress turbulence closures with no wall damping," *Bull. Am. Phys. Soc.*, Vol. 39, 1994, p. 1911.

37. Bardina, J., Ferziger, J. H. and Reynolds, W. C., "Improved turbulence models based on large-eddy simulation of homogeneous, incompressible turbulent flows," *Stanford University Technical Report No. TF-19*, 1983.

38. Johnston, J. P., Halleen, R. M. and Lezius, D. K., "Effects of a spanwise rotation on the structure of two-dimensional fully-developed turbulent channel flow," *J. Fluid Mech.*, Vol. 56, 1972, pp. 533-557.

39. Speziale, C. G. and Ngo, T., "Numerical solution of turbulent flow past a backward facing step using a nonlinear $K - \varepsilon$ model," *Int. J. Eng. Sci.*, Vol. 26, 1988, pp. 1099-1112.

40. Kim, J., Kline, S. J. and Johnston, J. P., "Investigation of a reattaching turbulent shear layer: Flow over a backward facing step," *ASME J. Fluids Eng.*, Vol. 102, 1980, pp. 302-308.

41. Eaton, J. K. and Johnston, J. P., "Turbulent flow reattachment: An experimental study of the flow and structure behind a backward facing step," *Stanford University Report No. MD-39*, 1980.

42. Durbin, P. A. and Speziale, C. G., "Local anisotropy in strained turbulence at high Reynolds numbers," *ASME J. Fluids Eng.*, Vol. 113, 1991, pp. 707-709.

43. Mellor, G. L. and Herring, H. J., "A survey of mean turbulent field closure models," *AIAA J.*, Vol. 11, 1973, pp. 590-599.

44. Daly, B. J. and Harlow, F. H., "Transport equations in turbulence," *Phys. Fluids*, Vol. 13, 1970, pp. 2634-2649.

45. Choi, K. S. and Lumley, J. L., "Return to isotropy of homogeneous turbulence revisited," in *Turbulence and Chaotic Phenomena in Fluids* (T. Tatsumi, ed.), pp. 267-272, North Holland, New York, 1984.

46. Lee, M. J. and Reynolds, W. C., "Numerical experiments on the structure of homogeneous turbulence," *Stanford University Technical Report No. TF-24*, 1985.

47. So, R. M. C., Lai, Y. G. and Hwang, B. C., "Second-order near-wall turbulence closures: A review," *AIAA J.*, Vol. 29, 1991, pp. 1819-1835.

48. Laufer, J., "Investigation of turbulent flow in a two-dimensional channel," *NACA TN 1053*, 1951.

49. Abid, R. and Speziale, C. G., "Predicting equilibrium states with Reynolds stress closures in channel flow and homogeneous shear flow," *Phys. Fluids A*, Vol. 5, 1993, pp. 1776-1782.

50. Tavoularis, S. and Karnik, U., "Further experiments on the evolution of turbulent stresses and scales in uniformly sheared turbulence," *J. Fluid Mech.*, Vol. 204, 1989, pp. 457-478.

51. Lee, M. J., Kim, J. and Moin, P., "Structure of turbulence at high shear rate," *J. Fluid Mech.*, Vol. 216, 1990, pp. 561-583.

52. Speziale, C. G., "Some interesting properties of two-dimensional turbulence," *Phys. Fluids*, Vol. 24, 1981, pp. 1425-1427.

53. Speziale, C. G., "Closure models for rotating two-dimensional turbulence," *Geophys. & Astrophys. Fluid Dyn.*, Vol. 23, 1983, pp. 69-84.

54. Schumann, U., "Realizability of Reynolds stress turbulence models," *Phys. Fluids*, Vol. 20, 1977, pp. 721-725.

55. Ristorcelli, J. R., Lumley, J. L. and Abid, R., "A rapid-pressure correlation representation consistent with the Taylor-Proudman theorem materially-frame-indifferent in the 2-D limit," *ICASE Report No. 94-1*, NASA Langley Research Center, 1994.

56. Haworth, D. C. and Pope, S. B., "A generalized Langevin model for turbulent flows," *Phys. Fluids*, Vol. 29, 1986, pp. 387-405.

57. Speziale, C. G., "Second-order closure models for rotating turbulent flows," *Q. Appl. Math.*, Vol. 45, 1987, pp. 721-723.

58. Speziale, C. G., "Turbulence modeling in non-inertial frames of reference," *Theoret. & Comput. Fluid Dyn.*, Vol. 1, 1989, pp. 3-19.

59. Shih, T. H. and Lumley, J. L., "Modeling of pressure correlation terms in Reynolds stress and scalar flux equations," *Cornell University Technical Report FDA-85-3*, 1985.

60. Shih, T. H. and Lumley, J. L., "Critical comparison of second-order closures with direct numerical simulations of homogeneous turbulence," *AIAA J.*, Vol. 31, 1993, pp. 663-670.

61. Speziale, C. G., Abid, R. and Durbin, P. A., "On the realizability of Reynolds stress turbulence closures," *J. Sci. Comp.*, Vol. 9, 1994, pp. 369-403.

62. Durbin, P. A. and Speziale, C. G., "Realizability of second-moment closure via stochastic analysis," *J. Fluid Mech.*, Vol. 280, 1994, pp. 395-407.

63. Speziale, C. G. and Gatski, T. B., "Assessment of second-order closure models in turbulent shear flows," *AIAA J.*, Vol. 32, 1994, pp. 2113-2115.

64. Bernard, P. S. and Speziale, C. G., "Bounded energy states in homogeneous turbulent shear flow – An alternative view," *ASME J. Fluids Eng.*, Vol. 114, 1992, pp. 29-39.

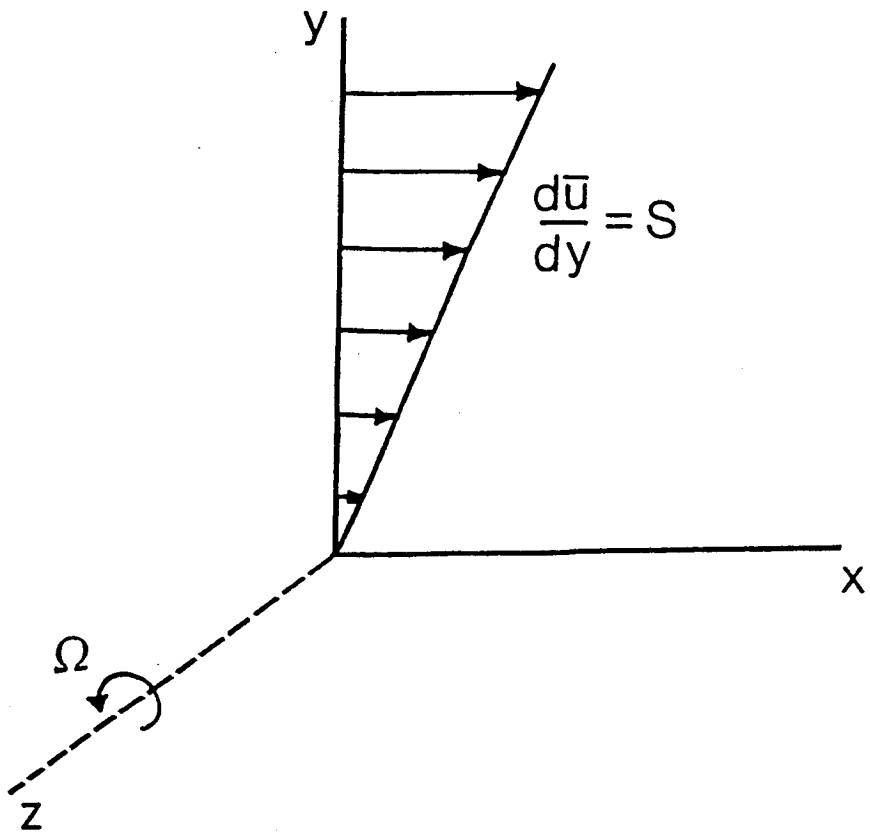

Figure 1. Schematic of homogeneous shear flow in a rotating frame.

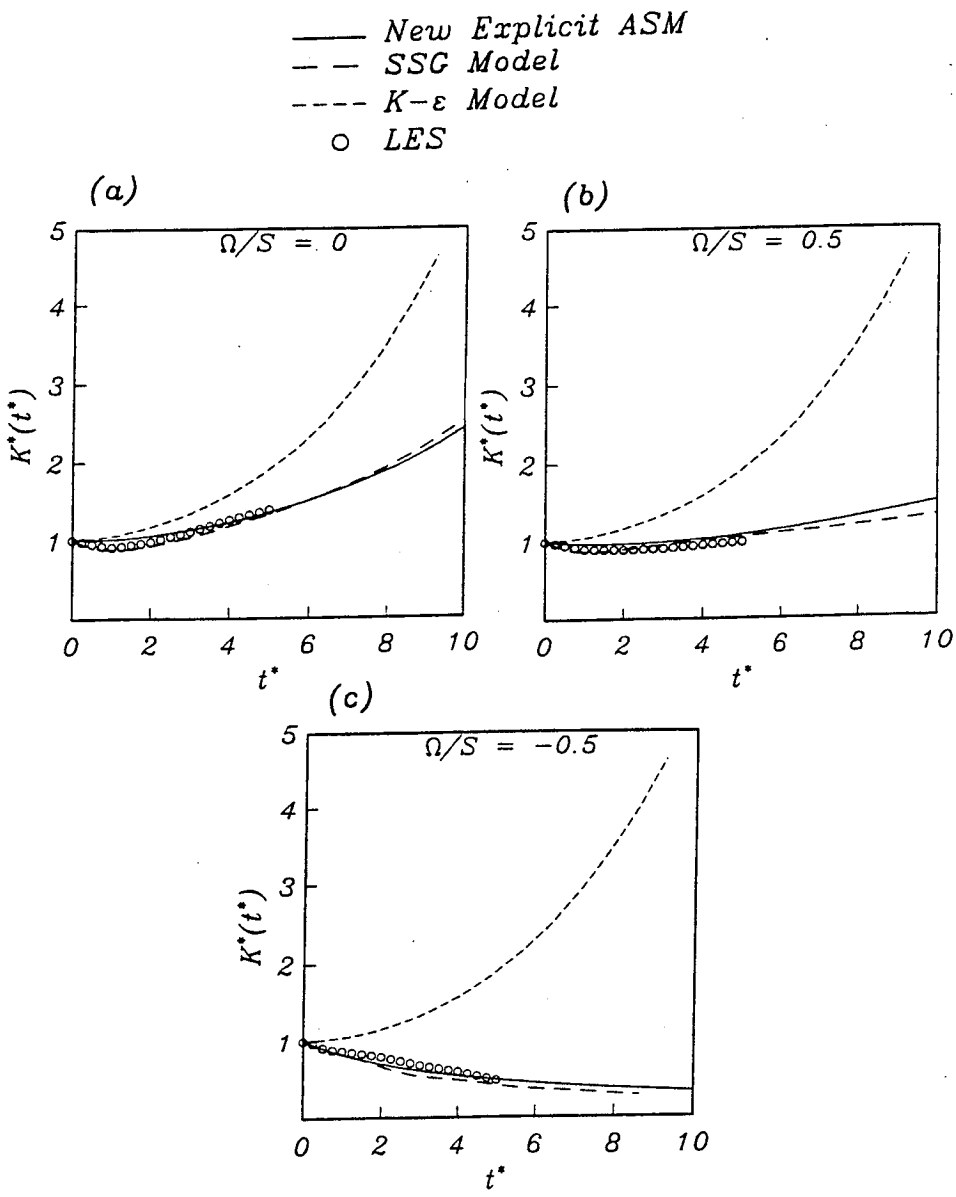

Figure 2. Time evolution of the turbulent kinetic energy in rotating homogeneous shear flow: Comparison of the model predictions with the large-eddy simulations of Bardina *et al.* [37]. (a) $\Omega/S = 0$, (b) $\Omega/S = 0.5$ and (c) $\Omega/S = -0.5$ (from Gatski and Speziale [3]).

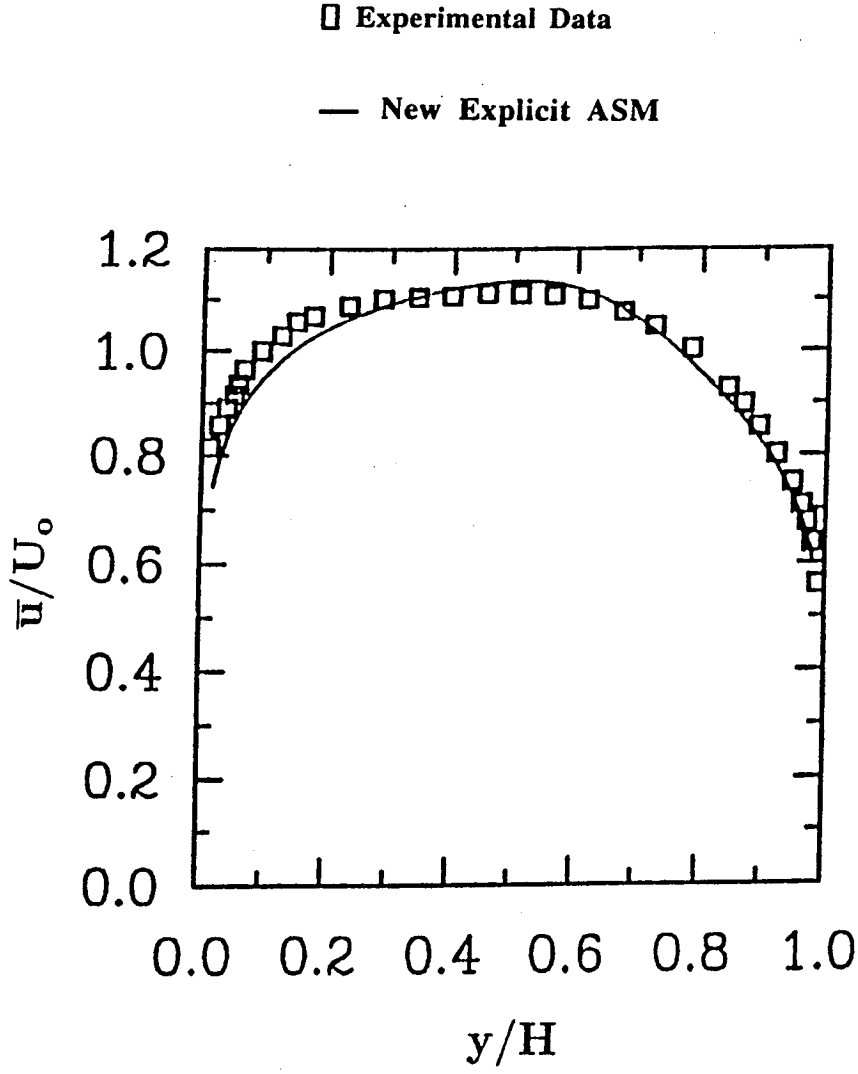

Figure 3. Comparison of the mean velocity profile in rotating channel flow predicted by the new explicit ASM of Gatski and Speziale [3] with the experimental data of Johnston, Halleen and Lezius [38].

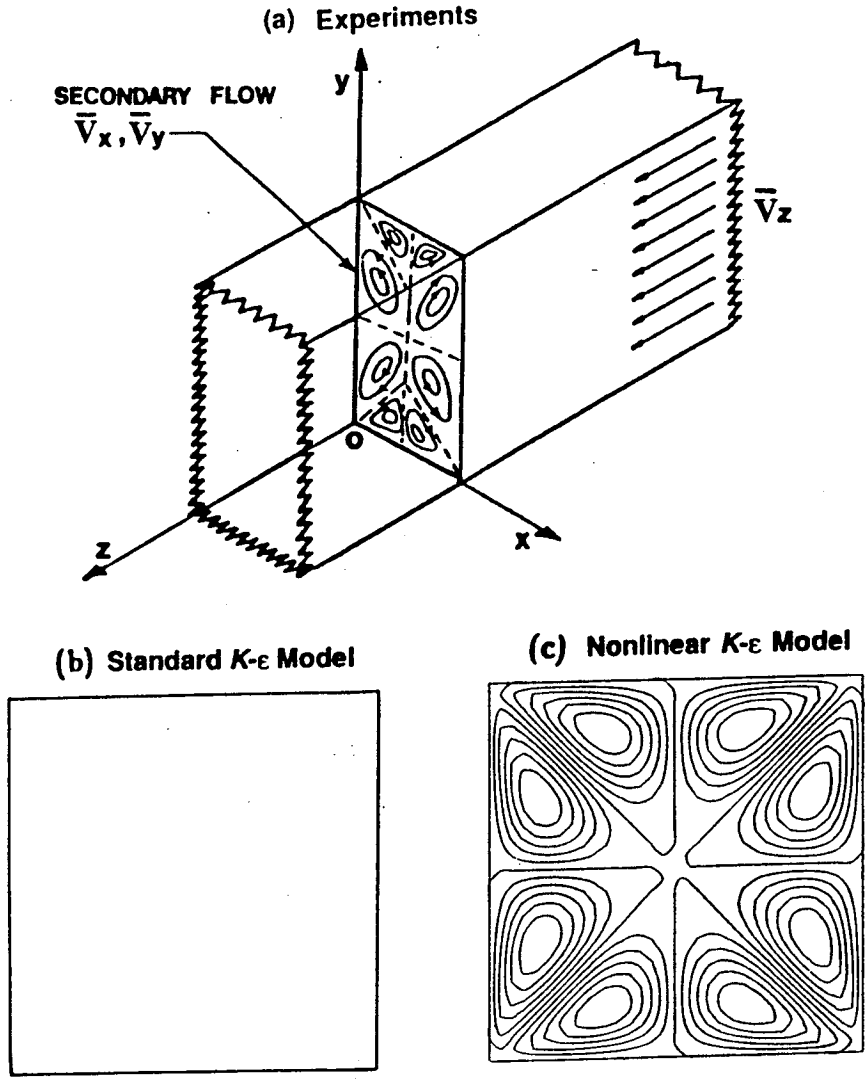

Figure 4. Turbulent secondary flow in a rectangular duct: (a) experiments, (b) standard $K-\epsilon$ model, and (c) nonlinear $K-\epsilon$ model of Speziale [22].

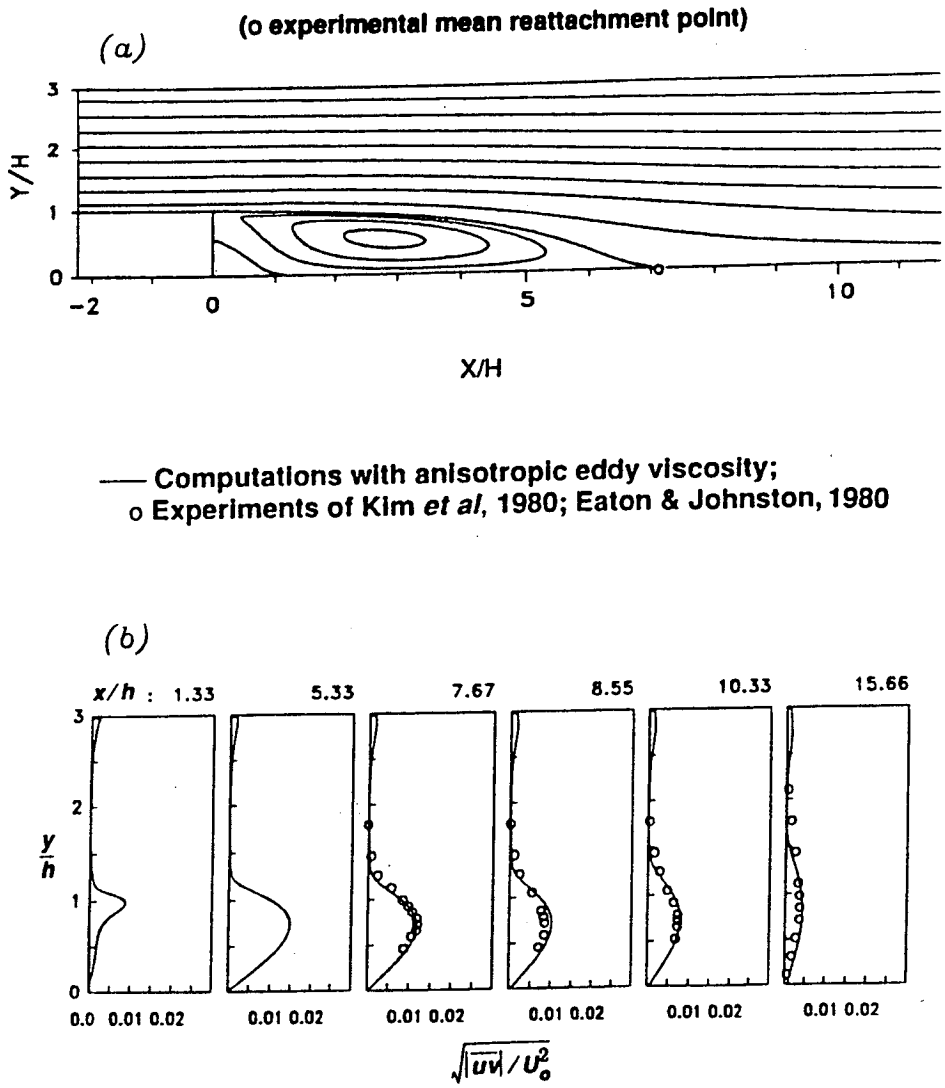

Figure 5. Turbulent flow past a backward facing step: comparison of the predictions of the nonlinear $K-\epsilon$ model [22] with experiments. (a) Streamlines and (b) turbulent shear stress profiles.

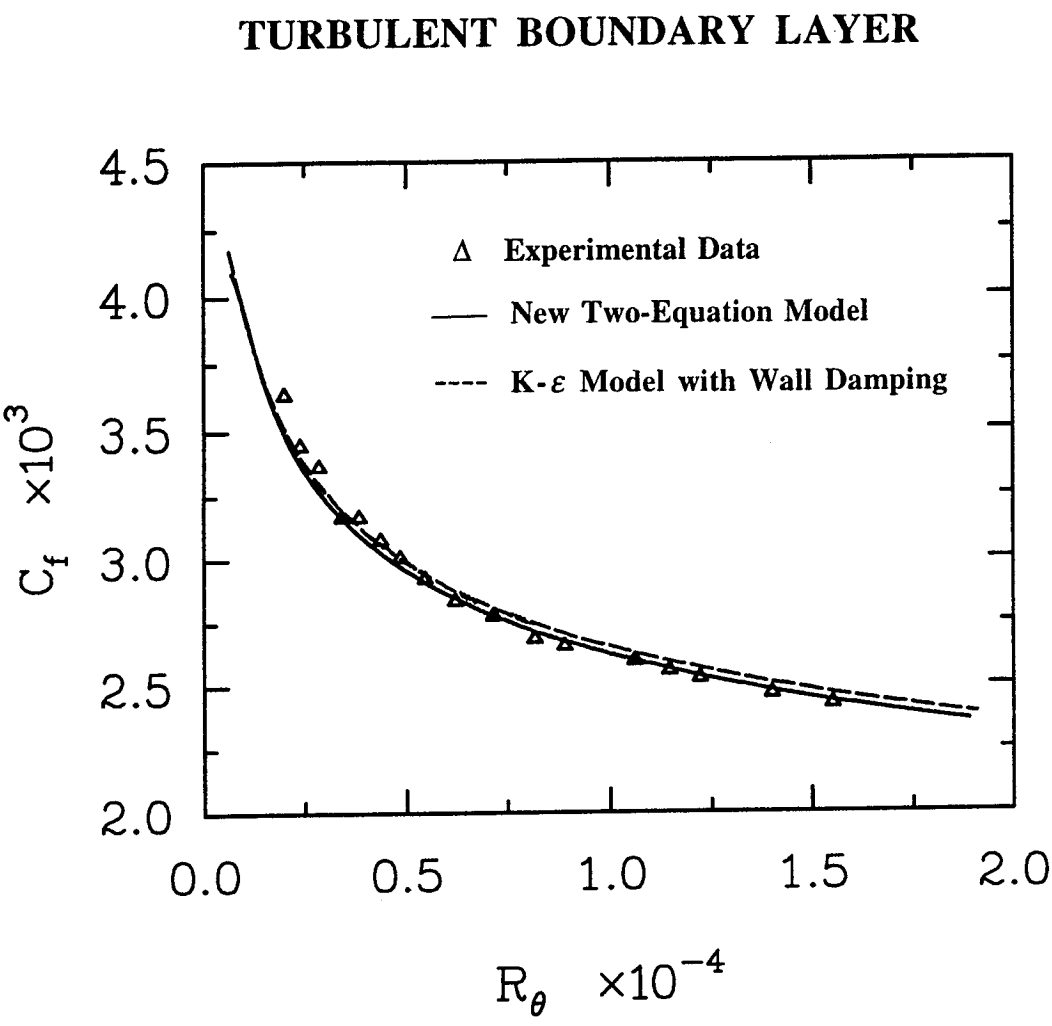

Figure 6. Comparison of the predictions of the explicit ASM of Gatski and Speziale [3] for skin friction with experimental data for the flat plate boundary layer (from Speziale and Abid [36]).

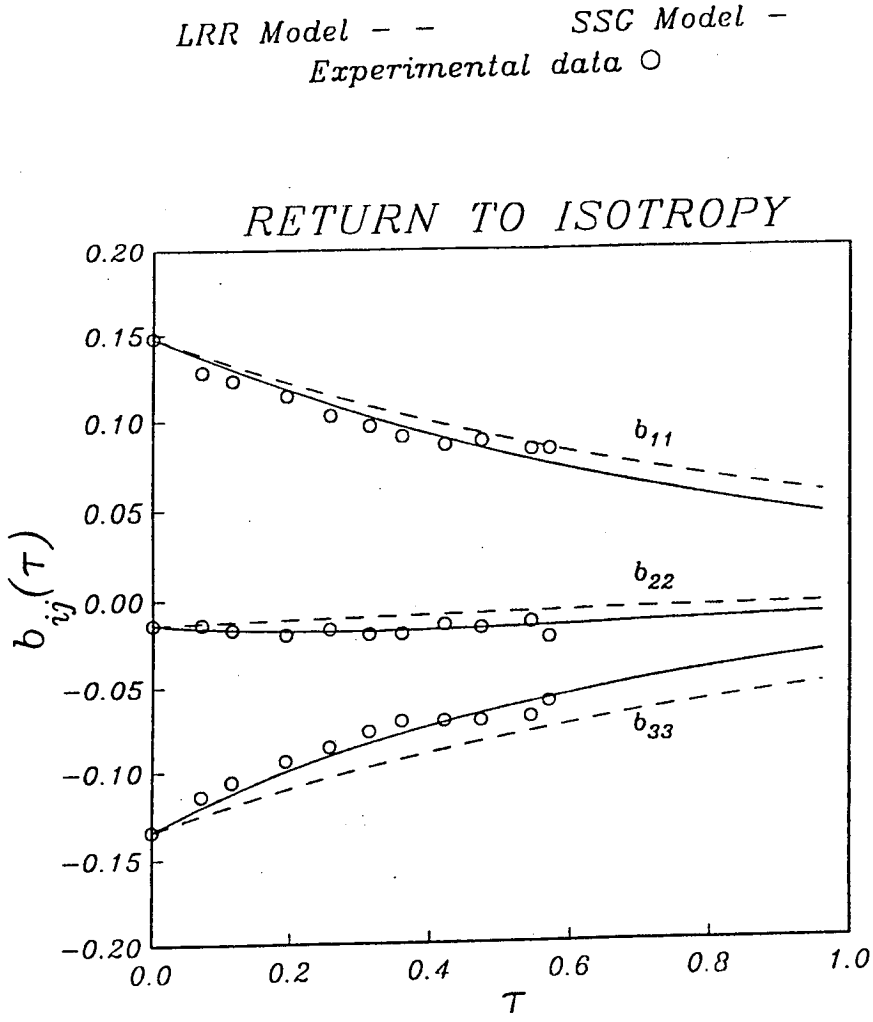

Figure 7. Time evolution of the anisotropy tensor in the return to isotropy problem. Comparison of the predictions of the LRR model and SSG model with the experiment of Choi and Lumley [45] (from Speziale, Sarkar and Gatski [2]).

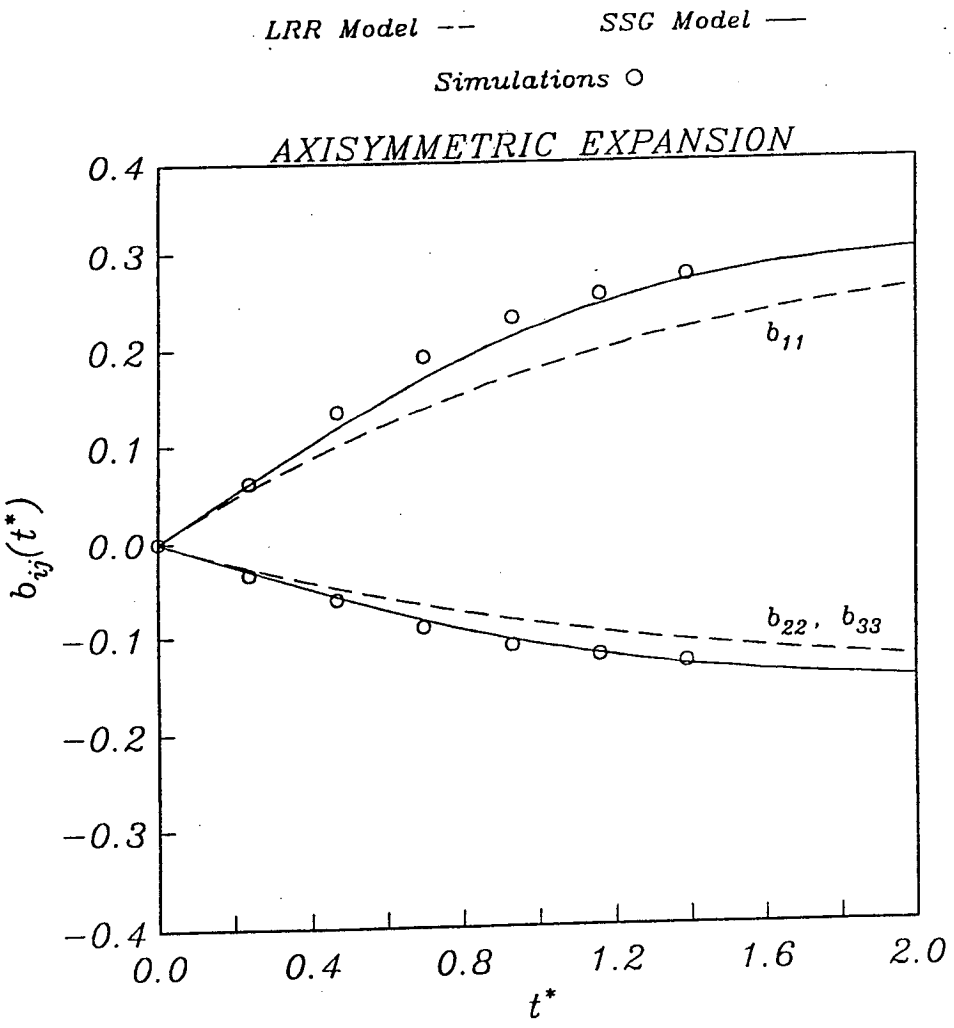

Figure 8. Time evolution of the anisotropy tensor in the axisymmetric expansion for $\varepsilon_0/\Gamma K_0 = 2.45$. Comparison of the predictions of the LRR model and SSG model with the direct simulations of Lee and Reynolds [46].

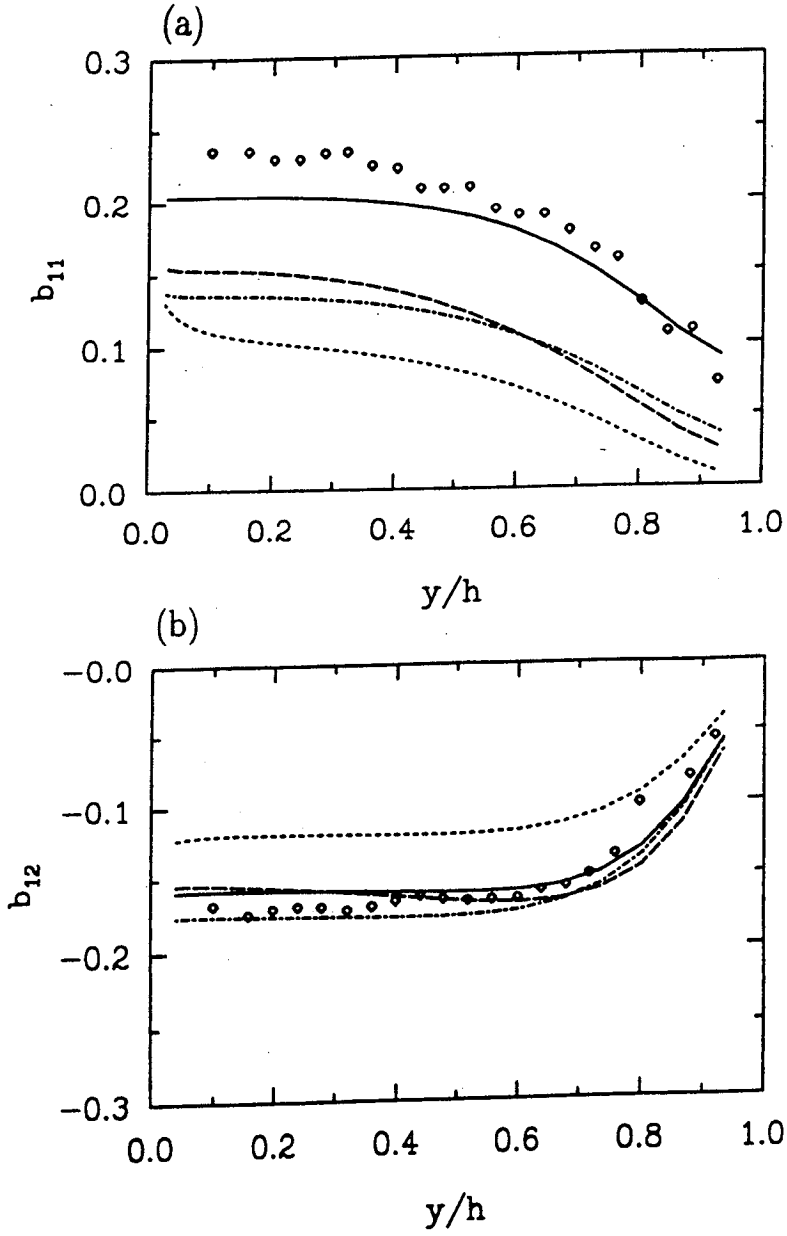

Figure 9. Comparison of full Reynolds stress calculations of channel flow with the experimental data ($\diamond$) of Laufer [48] for $Re = 61,600$. —— SSG model; – – – FLT model; – · – LRR model; and - - - SL model. (a) b_{11} component and (b) b_{12} component (from Abid and Speziale [49]).

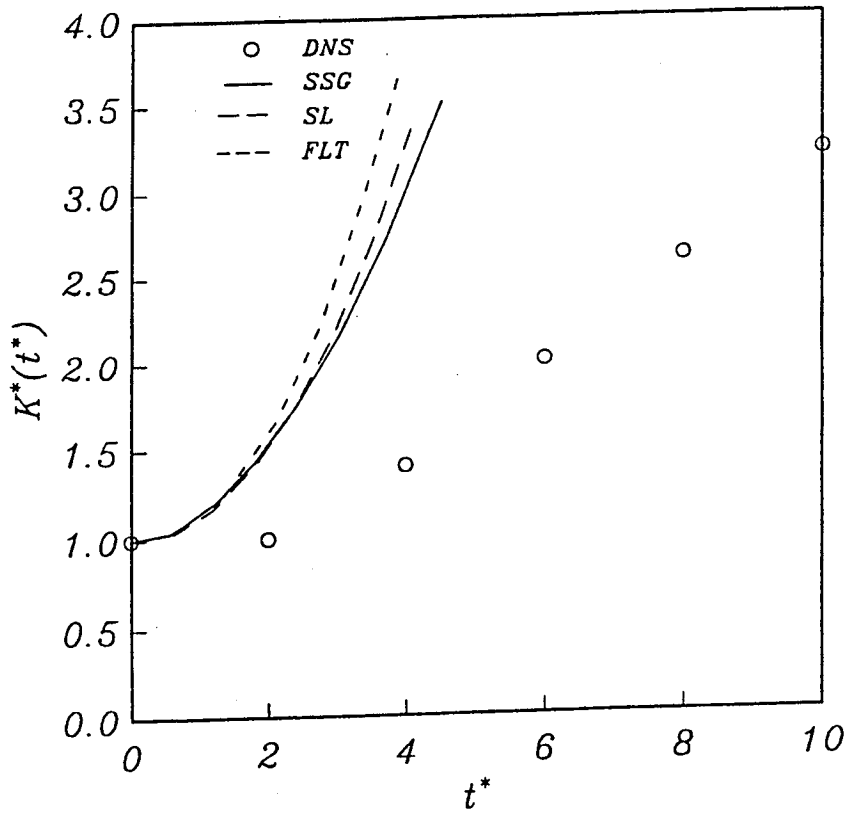

Figure 10. Comparison of the SSG, SL and FLT model predictions for the time evolution of the turbulent kinetic energy with the DNS results of Lee, Kim and Moin [51] for homogeneous shear flow ($SK_0/\epsilon_0 = 50$).

REPORT DOCUMENTATION PAGE

Form Approved
OMB No. 0704-0188

1. AGENCY USE ONLY(Leave blank)	2. REPORT DATE	3. REPORT TYPE AND DATES COVERED
	March 1995	Contractor Report

4. TITLE AND SUBTITLE
A REVIEW OF REYNOLDS STRESS MODELS FOR TURBULENT SHEAR FLOWS

5. FUNDING NUMBERS
C NAS1-19480
WU 505-90-52-01

6. AUTHOR(S)
Charles G. Speziale

7. PERFORMING ORGANIZATION NAME(S) AND ADDRESS(ES)
Institute for Computer Applications in Science
and Engineering
Mail Stop 132C, NASA Langley Research Center
Hampton, VA 23681-0001

8. PERFORMING ORGANIZATION REPORT NUMBER
ICASE Report No. 95-15

9. SPONSORING/MONITORING AGENCY NAME(S) AND ADDRESS(ES)
National Aeronautics and Space Administration
Langley Research Center
Hampton, VA 23681-0001

10. SPONSORING/MONITORING AGENCY REPORT NUMBER
NASA CR-195054
ICASE Report No. 95-15

11. SUPPLEMENTARY NOTES
Langley Technical Monitor: Dennis M. Bushnell
Final Report
To appear in the Proceedings of the 20th Symposium on Naval Hydrodynamics

12a. DISTRIBUTION/AVAILABILITY STATEMENT
Unclassified–Unlimited

Subject Category 34

12b. DISTRIBUTION CODE

13. ABSTRACT *(Maximum 200 words)*
A detailed review of recent developments in Reynolds stress modeling for incompressible turbulent shear flows is provided. The mathematical foundations of both two-equation models and full second-order closures are explored in depth. It is shown how these models can be systematically derived for two-dimensional mean turbulent flows that are close to equilibrium. A variety of examples are provided to demonstrate how well properly calibrated versions of these models perform for such flows. However, substantial problems remain for the description of more complex turbulent flows where there are large departures from equilibrium. Recent efforts to extend Reynolds stress models to non-equilibrium turbulent flows are discussed briefly along with the major modeling issues relevant to practical Naval Hydrodynamics applications.

14. SUBJECT TERMS	15. NUMBER OF PAGES
Turbulent Shear Flows; Reynolds Stress Modeling; Second-Order Closures; Two-Equation Models	44
	16. PRICE CODE A03

17. SECURITY CLASSIFICATION OF REPORT	18. SECURITY CLASSIFICATION OF THIS PAGE	19. SECURITY CLASSIFICATION OF ABSTRACT	20. LIMITATION OF ABSTRACT
Unclassified	Unclassified		

NSN 7540-01-280-5500

Standard Form 298(Rev. 2-89)
Prescribed by ANSI Std. Z39-18
298-102